Session E3

# Dynamic Testing and Analysis
# Essais dynamiques et analyse
# Dynamische Versuche und Berechnung

Leere Seite
Blank page
Page vide

# Stabilization of a Cable-Stayed Footbridge

Stabilisation d'une passerelle haubanée

Stabilisierung einer Schrägseil-Fussgängerbrücke

**Mykhailo L. KAZAKEVYCH**
Professor
Univ. of Railway Transport Eng.
Dnipropetrovsk, Ukraine

Mykhailo Kazakevych, born 1939, was involved for 25 years in problems of dynamics, aerodynamics and theory of vibration damping of structures. Author of many books and papers, he is currently Head of Structural Engineering Department at the University.

**Volodymyr V. KULYABKO**
Associate Professor
Institute of Civil Engineering
Dnipropetrovsk, Ukraine

Volodymyr Kulyabko, born 1938, has been engaged in research of dynamic problems of buildings, structures and machines. He presently works in the Department of Structural Mechanics of the Institute.

## SUMMARY

Methods of determining dynamic characteristics and natural frequencies of bridges are discussed, with the example of a cable-stayed pedestrian bridge in Vilnius, Lithuania. Vibration resonance in the horizontal plane was effectively eliminated by stiffening the bridge girders with added inclined cables.

## RÉSUMÉ

Les méthodes de calcul des vibrations naturelles de ponts sont présentées dans le cas d'une passerelle piétonnière haubanée à Vilnius, Lithuanie. Une stabilisation efficace, permettant d'éviter une résonance horizontale est obtenue au moyen de haubans additionnels.

## ZUSAMMENFASSUNG

Ein Verfahren zur Bestimmung der Eigenschwingungen der Brücken werden am Beispiel einer Schrägseil-Fussgängerbrücke in Vilnius, Lithauen, diskutiert. Durch Anordnung zusätzlicher Stabilisationskabel wurden Resonanzschwingungen der Brücke in der horizontalen Ebene vermieden.

## 1. INTRODUCTION

The cable-stayed footbridge across the river Neris in Vilnius, Lithuania, was built in 1984. The bridge was designed by the Transmost Institute in St. Petersburg (then Leningrad), Russia.

Structures of this type are rather sensitive to dynamic effects, especially moving pedestrian loading, which is characterized by periodic load pulses with a frequency of about 2 ± 0.2 Hz in the vertical direction and 1 ± 0.1 Hz in the horizontal plane [1]. Resonance oscillations occur when natural frequencies of the structure in the vertical or the horizontal plane coincide with the frequency of loading impulses.

In this case users complained about feelings of discomfort when crossing the footbridge. Review of the design calculations revealed that no dynamic analysis had been performed. Tests on the structure proved the existence within its natural frequency spectrum of a horizontal frequency of about 1 Hz. This indicated the need for stabilization of the bridge in the horizontal plane, which could be best achieved by modifying the horizontal rigidity and the associated horizontal natural frequency of the bridge to preclude resonance.

## 2. DESCRIPTION OF THE STRUCTURE

The footbridge is a three-span structure with span lengths of 118.5 + 51.0 + 34.5m (Fig. 1). Its cable stays, supported by the 47m high reinforced concrete pylon, are located in the central vertical plane of the bridge. Each of the four stays consists of six wire ropes made of 91 parallel galvanized wires of 5mm diameter.

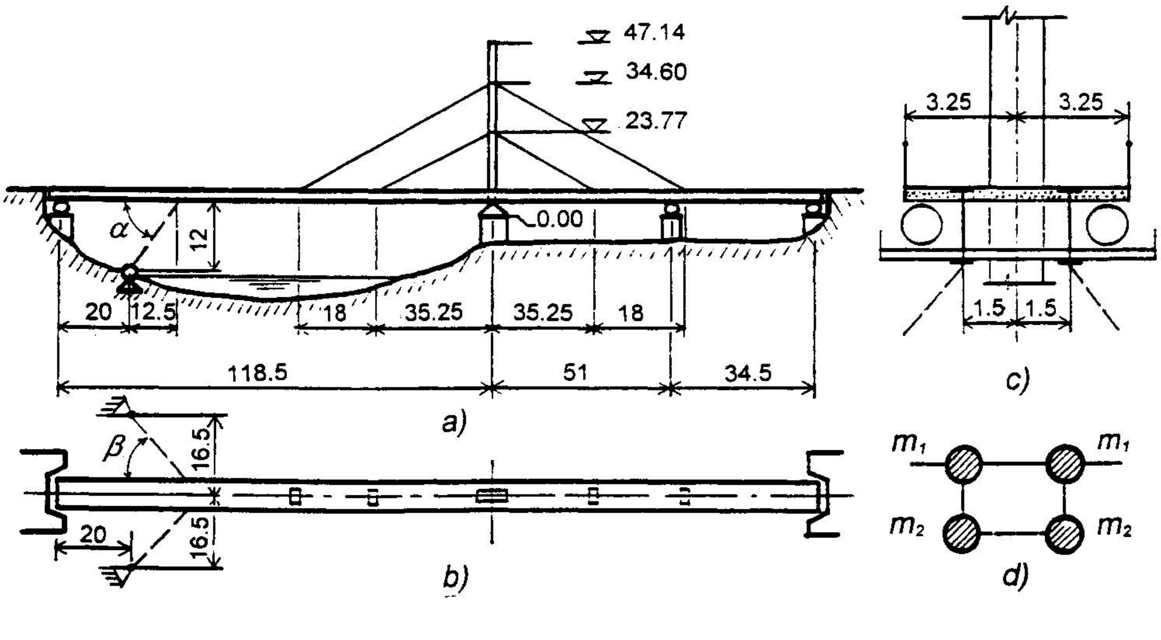


*Fig. 1. Cable-stayed pedestrian bridge in Vilnius, Lithuania. a) Elevation; b) Plan; c) Cross Section; d) Calculation model of the cross section.*

The 2.5m deep main girders are spaced at 3.0m. The girders have fixed bearings at the tower pier and expansion bearings at all other supports. The roadway width is 6.5m between the railings.

The bridge was designed for a pedestrian load of 400 kg/m and the weight of two hot water pipelines at 1700 kg/m.

## 3. DYNAMIC INVESTIGATIONS

### 3. 1. Determination of natural frequencies

The purpose of dynamic analysis is to obtain the lowest natural frequencies for the various vibration modes of the structure. Then the effect of pedestrian loading intensity on the values of natural frequencies and the various methods of modifying the vibration characteristics of the structure can be studied.

A discrete-continuous model with 46 degrees of freedom was used for the dynamic analysis by the finite element method. Longitudinal deformations of the elements and the asymmetry of the mass and the rigidity distribution along the depth of the bridge cross section were considered. The mass was assumed localized at four points of the cross section (Fig. 1 d).

The five characteristic vibration modes and the values of corresponding frequencies are shown in Fig. 2, arranged in order of increasing frequencies.

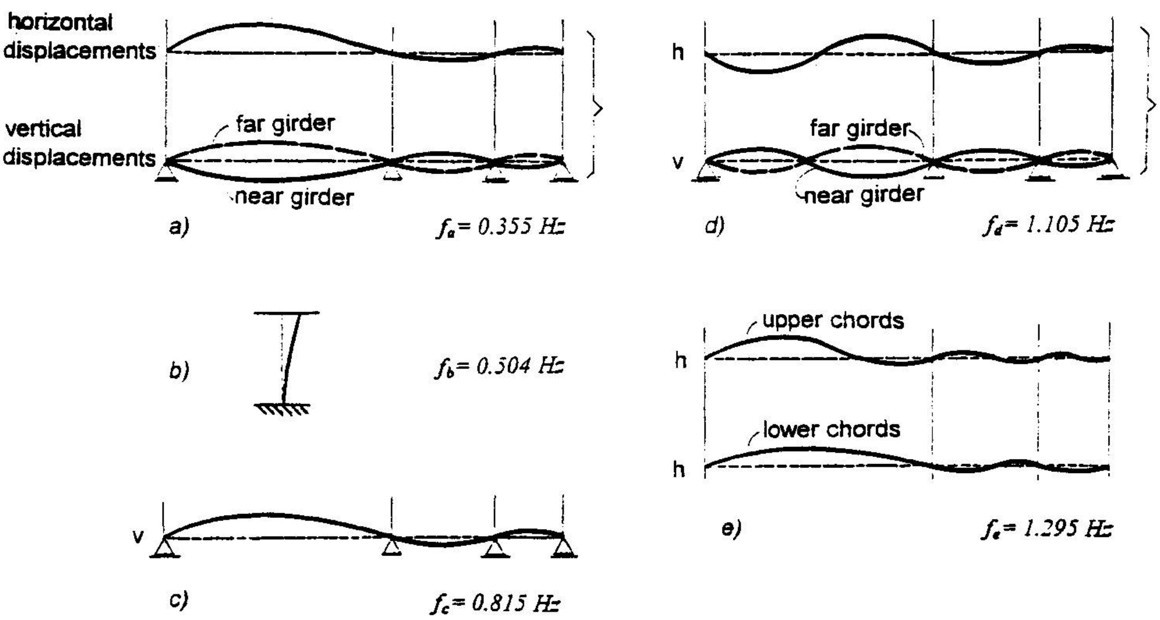


*Fig. 2. Vibration modes and natural frequencies of the bridge without pedestrian loading. a) flexural-torsional horizontal vibrations, first mode; b) lateral vibrations of the bridge pylon; c) vertical vibrations of the span; d) and e) second and third modes of the flexural-torsional horizontal vibrations.*

The lowest frequency was obtained for the first mode of the flexural-torsional horizontal vibrations (a). The lateral vibration out of the bridge plane is second lowest (b). Next is the vertical vibration of the span structure together with the pylon vibration in the longitudinal plane (c). Coupled flexural-torsional horizontal vibrations in the second and the third modes (d), (e) have the highest frequencies. The characteristic relationships between the torsional and the flexural horizontal vibrations of the structure are governed by the existence of only one (vertical) symmetry axis of the bridge cross section.

### 3. 2. Effect of pedestrian loading on dynamic characteristics

Dynamic effects on the bridge are governed by two characteristic properties of moving pedestrian loading:

a) the frequency $f$ the load impulses depends on the intensity $q$ of the pedestrian loading;

b) the velocity $V$ of pedestrian movement along the bridge also depends on the load intensity $q$.

These relationships were determined by numerous investigations by I. I. Kazej, S. I. Kazej, A. L. Zakora and M. I. Kazakevych and can be expressed by the following formulas:

$$q = \frac{400}{1 + 1.4f}, \quad kg/m^2$$

$$V = 0.036\,(25f^2 + 30f), \quad km/h$$

The relationships between the pedestrian load intensity, the velocity of the pedestrians' movement and the frequency of the load impulses are shown graphically in Fig. 3.

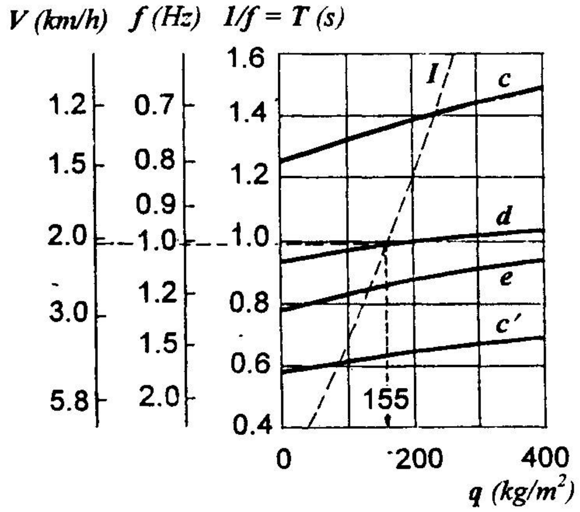


*Fig 3. Graphic representation of relationships between the footbridge frequencies f, velocity of pedestrian movement V, and pedestrian loading intensity q for relevant vibration modes shown in Fig. 2.*
*c) vertical vibrations, 1st mode;*
*c) vertical vibrations, 2nd mode;*
*d) flex.tors. horiz. vibr. 2nd mode;*
*e) flex.tors. horiz. vibr., 3rd mode;*
*I) interaction curve.*

Inspection of this diagram shows the unfavorable coincidence of the horizontal frequency of the pedestrians' effect with the natural frequency of 1.02 Hz of the flexural-torsional horizontal vibrations of the second mode, which occurs when the average velocity of the pedestrians' walk $V$ is about 2.05 km/h. This case corresponds to the pedestrian load $q = 155\ kg/m^2$, or an average of 2.21 pedestrians per one square meter of the bridge deck. This explains the pedestrians' discomfort described as "the ground slipping from under the feet".

### 3.3. Comparison of analytical and experimental results

Ground rules for analytical diagnostic investigations of dynamic behavior of bridge structures under service conditions as well as during the erection have been outlined in [2]. Dynamic characteristics can also be obtained directly, by tests on the completed structure. The methods for dynamic testing of bridges are described in detail in [3]. The relevant factors in such investigations are: the wind effects, vibrations induced by vehicular traffic which may magnify the natural vibrations of the structure, dynamic characteristics of pedestrian loading. Experimental methods, which can provide verification of analytical results, are generally more reliable.

Comparison of dynamic characteristics obtained by the two methods for the Vilnius bridge is given in Table 1.

| Case (refer to Fig. 2) | Analysis | Tests |
|---|---|---|
| a) flexural-torsional horizontal vibrations, 1st mode | 0.355 | 0.37 |
| b) pylon vibrations out of the bridge plane | 0.504 | - |
| c) vertical vibrations, 1st mode | 0.815 | 0.83 |
| d) flexural-torsional horizontal vibrations, 2nd mode | 1.105 | 1.20 |

***Table 1.*** *Calculated and experimental values of vibration frequencies (Hz)*

The comparison shows good qualitative agreement between the analytical and the experimental results, however, the values of frequencies obtained by testing are consistently higher by about 3 - 5%.

Dynamic testing also provided data for determination of the damping characteristics of the structure. For vertical oscillations the logarithmic decrement value of damping $\delta$ was found to be 0.033; for the flexural-torsional horizontal oscillations the value of $\delta$ was 0.017 to 0.04.

## 4. STABILIZATION OF THE BRIDGE

The bridge is one of the access routes to the well frequented Vinginis Park in Vilnius; therefore pedestrian comfort, in addition to fatigue strength of the structure, were important considerations.

Investigations established the need to increase the flexural-torsional horizontal vibration frequency of the second mode (case (d) in Fig. 2) in order to preclude resonance. Two methods of achieving this aim were considered:

1. Increase of the horizontal rigidity of the bridge by means of two additional girders to be placed outside of the existing ones;

2. Increase of the horizontal rigidity by means of added cable stays.

Based on considerations of structural effectiveness, economy, construction problems and maintainability the second alternative was chosen.

Added cable stays with Angles of inclination $\alpha = 44°$ and $\beta = 53°$ are attached to the bottom flanges of the girders at a point 32.5m from the end support (Fig. 1). The lower ends of the cables are anchored in special foundation blocks in the flood plane of the river.

The lower cable ends are provided with spring absorbers having longitudinal natural frequency of 10 Hz, with the purpose of stabilizing the vertical displacement of the span under the effects of temperature and pedestrian loading.

By these means the frequency of the second mode flexural-torsional horizontal vibrations of the structure, which was causing resonant vibrations under the effects of pedestrian loading, was increased by 20% and the problem was eliminated.

## REFERENCES:


1. Schulse, H. "Dynamische Einflüsse der Verkehrslast auf Fussgängerbrücken. *Signal and Schiene,* 1980, No. 2, p. 91-93; No. 3, p. 143-147.

2. Kazakevych, M. I., Kulyabko, V. V. "Complex Study of Dynamics and Aerodynamics of Long-span Pipelines and Bridges". *East European Conference on Wind Engineering,* Warsaw, 4-8 July 1994, p. 113-122.

3. Kazakevych, M. I. "Aerodynamics of Bridges". Transport, Moscow, 1987.

# Continuous Load and Condition Monitoring of a Highway Bridge

Surveillance continue de l'état et des charges d'un pont autoroutier

Dauerüberwachung für die Belastungs- und Zustandsbeobachtung einer Autobahnbrücke

**Werner F. RÜCKER**
Fed. Inst. for Material
Research and Testing (BAM)
Berlin, Germany

**Samir SAI**
Fed. Inst. for Material
Research and Testing (BAM)
Berlin, Germany

**Rolf G. ROHRMANN**
Fed. Inst. for Material
Research and Testing (BAM)
Berlin, Germany

**Wolfgang SCHMID**
Fed. Inst. for Material
Research and Testing (BAM)
Berlin, Germany

## SUMMARY

The maintenance of structures and the protection of their serviceability requires a profound knowledge not only of their actual but also of their prospective condition. Consequently, it is convenient to observe the structure's conditions by means of permanent monitoring systems measuring all important parameters which can influence the structure's behaviour. Only the continuous and simultaneous measurement and control of certain data, like traffic loads, temperature distributions, etc., and their effect on the main structural parameters, provide for a reliable interpretation of changes in the structures behaviour.

## RÉSUMÉ

Une bonne conservation des ouvrages et le maintien de leur aptitude au service exige non seulement une connaissance précise de leur état actuel mais aussi de leur fonctionnement futur. Cela implique une surveillance continue qui peut être réalisée aujourd'hui à l'aide de techniques modernes de mesures et d'évaluation. Seul le contrôle continu et simultané de différentes valeurs ayant une influence sur les paramètres principaux d'un ouvrage, par exemple les charges de trafic et les répartitions de température, permet d'interpréter de façon sûre les dégradations susceptibles de se manifester.

## ZUSAMMENFASSUNG

Für die Erhaltung von Bauwerken und zur Sicherung ihrer Funktionsfähigkeit ist es notwendig, eine genaue Kenntnis sowohl des aktuellen als auch des künftigen Bauwerkszustandes zu haben. Dies ist eine Aufgabe der Dauerüberwachung, die heute unter annehmbaren Aufwand mit Hilfe moderner Meß- und Auswerttechniken durchführbar wird. Erst die gleichzeitige und kontinuierliche Beobachtung, Messung und Kontrolle verschiedenster Einflussgrössen auf relevante Bauwerksparameter, wie zum Beispiel Verkehrslasten und Temperaturverteilungen, ermöglichen eine sichere Interpretation von sich ankündigenden Zustandsänderungen.

## 1. INTRODUCTION

The guarantee of the functioning and serviceability of constructions, which are subject to the changing service loads and functional behaviour, where certain external effects are not predictable or the real bearing capacity ist not exactly known, is a very ambitious task. One contribution to solve this problem is to observe and assess permanently the loading and the condition of the structure by using automatically operating monitoring systems. In recent years at BAM Berlin such a system was developed and tested. In this paper the conception of the system and the kind of installation at a highway bridge in Berlin, Germany, is described and first results received with this system are presented.

## 2. CONCEPTION

The main task for the mission of a monitoring system is to extend the service time of a structure. To meet this aim amplitude and duration of the service loads will be observed continously. Based on this data possible changes of material properties which are not directly observable can be predicted using static and dynamic stress models. Beyond that the alteration of the structure, that is the decrease of bearing capacity, modification in the static system due to internal and external effects, corrossion etc. can be assessed by measuring static and quasistatic deformations, amplitudes of vibration, eigenvalues and mode shapes and the increase of known damages like cracks on certain positions at the structure. Results received from the monitoring data which will enable repair work at an early stage will extend the service life of the structure and give more security of the functional behaviour and load bearing capacity.

The monitoring system records the real loadings of the traffic. The results are given as load distribution functions. These are the data basis for the evaluation of load models, by which the fatique life of the structure can be computed by using well-known fatique models. The dynamic components of the traffic loads increase the level of loading and reduce the service life time due to fatique effects. The dynamic loading components are recorded in terms of the so-called dynamic factor, which is defind by $\varphi = \varepsilon_{stat+dyn} / \varepsilon_{stat}$.
Since the number of sensors for such measurements is limited, it is very important to know the location of maximum stress of the considered constructions. It is convenient to use modal analysis techniques for this purpose. First of all the eigenfrequencies $f_i$ which are excited mostly by the traffic passing over the bridge have to be identified by means of long-term measurements due to the bridge's vibration. When these frequencies are known the modal shapes $w_i$ belonging to $f_i$ will be determined by an experimental modal analysis under artifical excitation. In certain cases it is also possible to extract modal shapes from measurements under traffic excitation. The areas of maximum stress can be evaluated by differentiating the modal shapes, using the relation $w_i''(x) \approx \varepsilon_i(x)$. It should be mentioned, that this approach requires sufficient close distances between the measurement points.

Observing and assessing the global state as well as local properties and possible changes of the structure is the main aim of conditional monitoring. Changes in the bearing capacity are normally caused by changes in the vital members of the structure due to cracks or changes in the support of the structure. Alteration of that kind modifies the dynamic behaviour of the structure, i.e. the modal parameters are changing. In order to detect changes in the structural behavior at an early stage relevant natural frequencies and related modal shapes are used as indicator values or functions. In [2] results are given which show that especially for statically

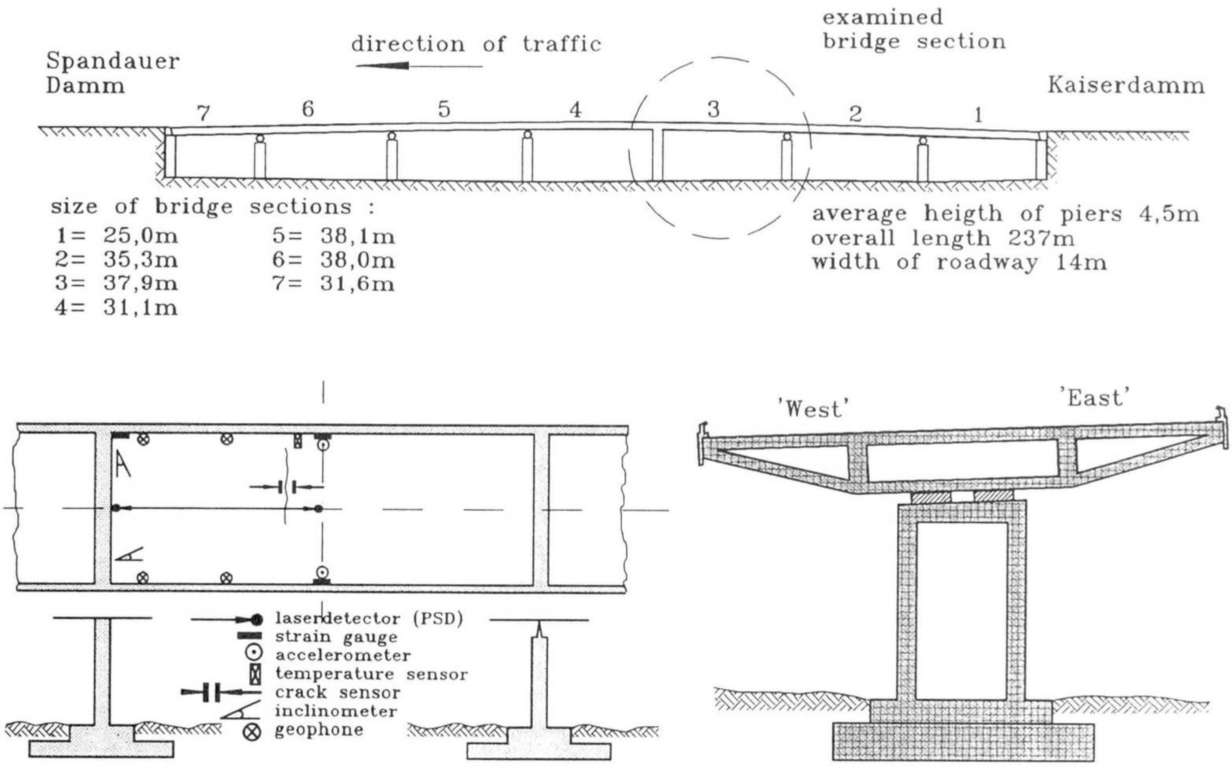


Figure 1: Highway Bridge Westend
Profile of the bridge (above), Location of sensors (left), Cross-section (right)

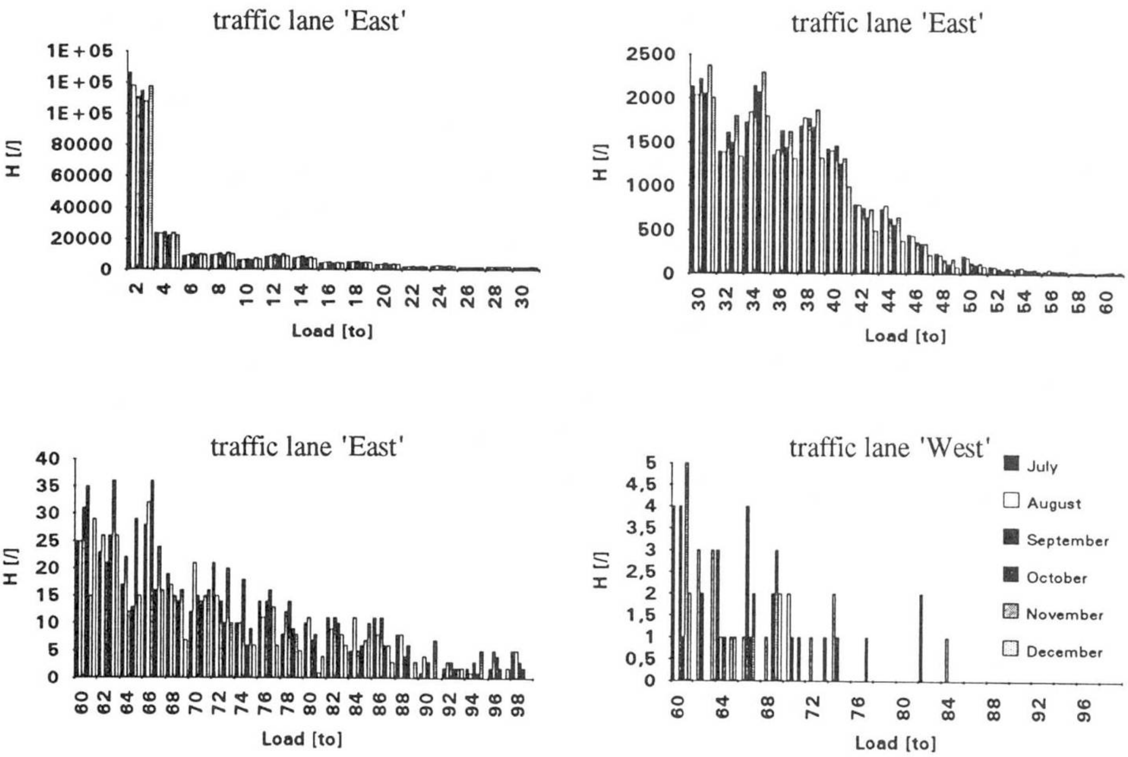


Figure 2: Frequency H of static traffic loads $P_{stat}$ from 6 months (July - December 1994)

indeterminated systems the modal shapes are much more sensitive indicating alteration of the structural behaviour then natural frequencies.
In order to record the influence of temperature variations to the static and dynamic behaviour of the bridge, two sensors measuring the structural temperature are also included in the monitoring system.

## 3. STRUCTURE AND SENSORS

This 30 year old prestressed bridge (figure 1) has had a lot of cracks occurring at the floor slab of the hallow box, at the cross girder above the columns and at the longitudinal main beams. There was no clear explanation for these cracks. So the supervising authority decided to repair the bridge first and then to install a monitoring system to surveille the bridge by measuring the service loads and the conditional behaviour permanently. Positions and types of 15 sensors attached inside the bridge is shown in figure 1. The traffic loadings are measured with strain gauges attached at the middle of the main beam and above a support.

## 4. RESULTS

From the amount of existing monitoring data some selected results will be discussed. At first we discuss the results of loading control. The common approach to simulate traffic loads, Riera et. al. described in [3], is a composition of assumptions about vehicle characteristics, mean velocities and traffic composition. In connection with a numerical model this loads result in desired dynamic responses. In our approach we directly measure the dynamic responses and then based on this data develope an artificial loading model for the bridge. Assuming linear conditions the bridge was calibrated first by measuring the maximum midspan strains at the girders of the described span due to a heavy truck of known weight travelling along the bridge on different lanes. The monitoring system then is measuring continously the loading conditions under normal traffic. Within a certain time window the maximum value of measured strains is stored. This will be done before and after a low pass filtering of the signal. In relation to the results of the calibration data each of these strain values belong to an artificial vehicle load due to each traffic lane. So in certain periods of time an averaged passage frequency classified by vehicle loads is developing, which is as stable as the measuring time is long enough. Figure 2 shows representative results of the load density function for a observation time of 6 months.
Long-time monitoring is able to show the monthly deviations of the load distributions. Comparing the results of figure 2 with those of the theoretical results in [3] a recognizeable difference is that the measured loads does not fulfill a normal distribution.

| vehicle loads [to] | West | East |
|---|---|---|
| 0 - 29 | 99.466 % | 94.35 % |
| 30 - 59 | 0.530 % | 5.55 % |
| 40 - 90 | 0.004 % | 0.10 % |
| total | 1209769 | 1255124 |

Table 1: The distribution H of the classified passages

The dynamic factor $\varphi$ is shown in figure 3. The distribution due to each respective loading class is different. Up to the value $\varphi = 1.25$ the relative frequency $H_r$ in each loading class and traffic lane is equal. For values $\varphi > 1.25$ on the traffic lane 'West' in comparison with

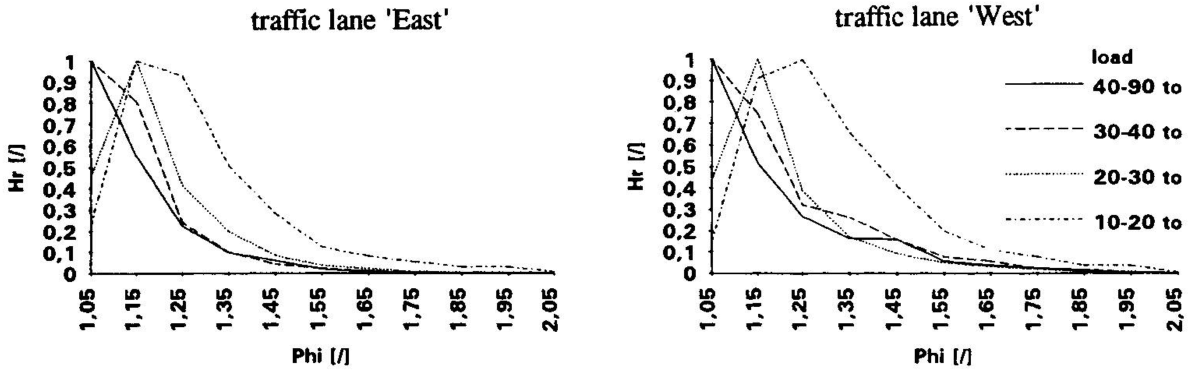


Figure 3: Relative frequency $H_r$ of the dynamic factor $\varphi$ measured during July 1994

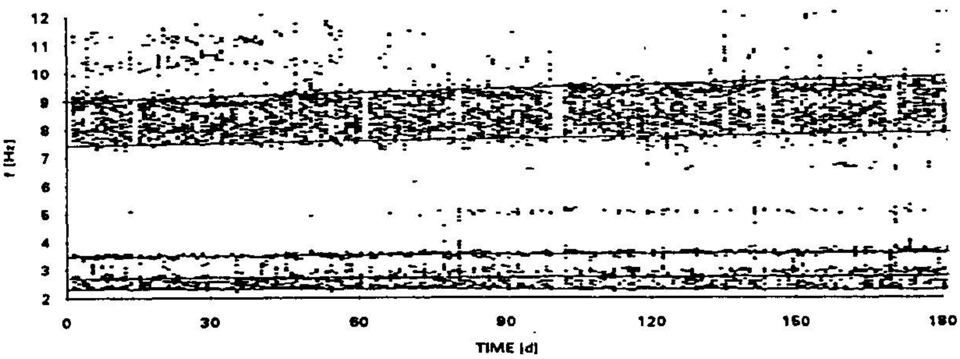


Figure 4: Dominant frequencies $f_i$ measured during t=6 months (July - December 1994)

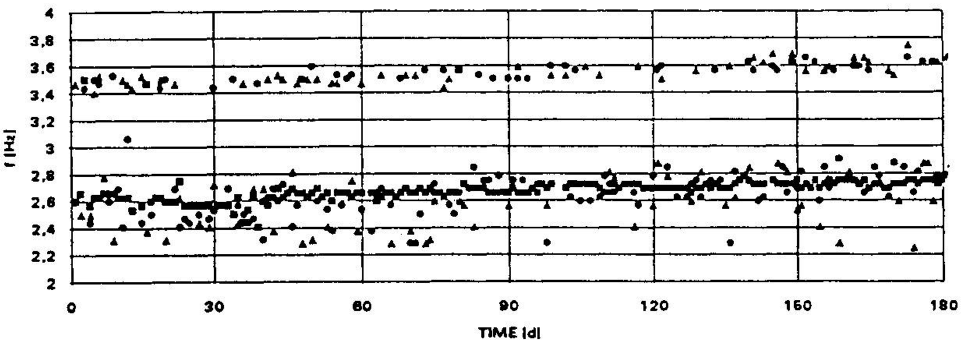


Figure 5: Changes of 2 natural frequencies $f_i$ of the bridge (zoomed from figure 4) due to temperature variations

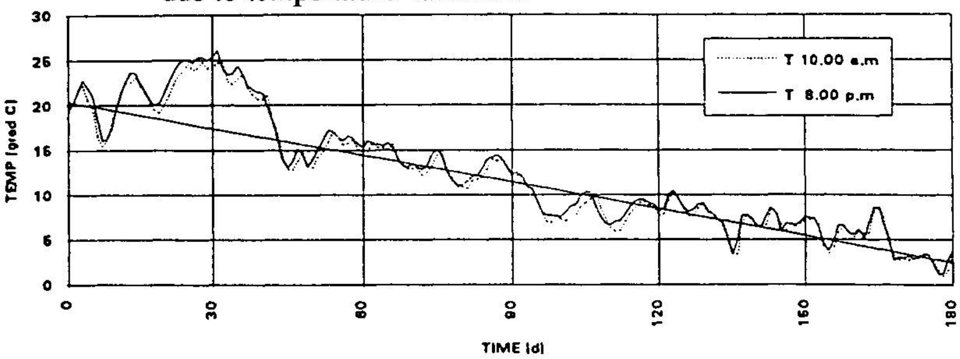


Figure 6: Structural temperature T measured during t=6 months (July - December 1994)

with 'East' (figure 3) we can find a greater amount of vehicles in all load classes with higher dynamic loading parts due to their higher velocities.

As part of the condition monitoring figures 7 and 8 present results of monitored changes of the natural frequencies at certain measurement points of the bridge. The approach of getting this results is measuring permanently the vibrations of the bridge, evaluating the frequency spectra and picking from that a certain amount of frequencies which belong to dominant amplitudes. Marking these frequencies daily in the diagram the results are presented in figure 4. In case of unchanged structural conditions natural frequencies can be detected as horizontal lines within the amount of all frequency points. The natural frequencies determined by means of modal analysis can also be identified but in a noisy environment.This effect is predominant the influence of the changing constitutions of traffic relating to bridge excitations. Figure 4 shows one of the results of condition monitoring during the period of 6 months. Here the values of the natural frequencies are increasing, what means that the structural stiffness is increasing. Zooming figure 4 into figure 5 this trend is visible as a linear function and will be caused by the change of the structural temperature (figure 6). The correlation between both indicates a relationship approximatly $\Delta f \cong 1/100 \cdot \Delta T$. The physical background of this effect is exactly not yet known, but the consequences are not negligible. Variations of the structural stiffness within an adjusted finite element model for the bridge have shown, that the difference $\Delta f = 0.2$ Hz of the natural frequencies $f_1$ and $f_2$ due to the change of the temperature between summer and winter corresponds to a change of stiffness of more than 50% of one whole span. This effect shows that monitoring additional environmential parameters is not of secondary significance.

## 5. CONCLUSIONS

This contribution introduces an automatically working monitoring system for loading and condition monitoring of bridges. The loading control includes determination and classification of equivalent vehicle loads outgoing from continously measured static and dynamic strains at the structure. The condition monitoring supplies criteria about the actual local and global structual conditions under the control of different sensitive parameters like deformations, dynamic quantities and environmential parameters. Results of the system which has been working since more than 2 years at a highway bridge in Berlin are presented.

## 6. REFERENCES

[1] DEGER,Y.; CANTIENI, R; PIETRZKO,S.; RÜCKER,W. ; ROHRMANN, R.G. :
Modal Analysis of a Highway Bridge : Experiment, Finite Element Analysis and Link
13 th IMAC, International Modal Analysis Conference, Nashville, USA, 1995

[2] ROHRMANN, R.G.; RÜCKER, W. :
Surveillance of Structural Properties of Large Bridges Using Dynamic Bridges
6th ICOSSAR, Intern. Conf. on Structural Safety and Reliability, Innsbruck, 1994

[3] RIERA, J. D.; ITURRIOZ, I. :
Simulation of Traffic Loads for Dynamics Analysis
6th ICOSSAR, Intern. Conf. on Structural Safety and Reliability, Innsbruck, 1994

# Traffic-Induced Vibrations on Structures

## Vibrations causées par le trafic sur les constructions

## Durch Verkehr verursachte Schwingungen an Bauten

**Paolo CLEMENTE**
Researcher
ENEA Casaccia
Rome, Italy

Paolo Clemente, born l959, received his civil engineering degree and his Ph.D. in structural engineering at the Univ. of Naples. Since 1985 he has been researcher at ENEA Casaccia and has worked in structural and earthquake engineering.

**SUMMARY**

The results of an experimental study carried out on several monuments in Rome are presented in this paper. The influence of the traffic-induced vibrations is investigated, especially with regard to the vibrations induced by the underground trains. An interesting solution used to preserve an ancient building in the centre of Rome is also discussed.

**RÉSUMÉ**

L'article présente les résultats d'une étude expérimentale sur différents monuments de Rome. L'effet des vibrations causées par le trafic a été analysé, spécialement celles provoquées par le métro. L'article présente aussi une méthode intéressante qui a été appliquée pour protéger un ancien bâtiment au centre de Rome.

**ZUSAMMENFASSUNG**

Der Bericht beschreibt die Ergebnisse von Untersuchungen einiger Denkmäler von Rom. Es wurden durch den Verkehr verursachte Schwingungen studiert, besonders die Schwingungen durch die Untergrundbahn. Der Artikel zeigt eine Lösung, die an einem alten Gebäude im Zentrum von Rom angewendet wurde.

## 1. INTRODUCTION

Traffic induced vibrations do not represent, in general, an immediate hazard to the structures but they can contribute, over the years, to their bad health status. This is certainly true for the constructions of the ancient cities, built when there was no traffic question. Examples of this kind are almost all the cities in Italy. Small streets, masonry buildings and often several monumental constructions, not preserved from the ambient around them, characterized them.
Traffic induced vibrations become very dangerous when acting on structures already damaged by earthquakes. Most of the architectural and monumental heritage in Italy live in this condition. In fact, it has suffered to various degrees during paste earthquakes, as described by historical documents [2, 3, 4]. On the other hand the strength of a structure under seismic actions can be deteriorated because of the continuous dynamic effects due to the traffic. Particularly dangerous are the vibrations due to the passing of the trains.
The first step in a preservation effort is the investigation of the health status of the structure. This can be performed by monitoring the construction in order to analyze their dynamic behaviour under both ambient and forced vibrations.
The results of an experimental study carried out on several monuments in Rome are shown in this paper. The research project was organized by the Italian Agency for New technologies, Energy and Environment (ENEA), in collaboration of the Archeological Commision of Rome. The measuraments were done by ISMES, on behalf of ENEA [7].
The effects of the traffic induced vibrations are investigated, especially with regards to the vibrations induced by the trains of the underground. The velocity amplitude and the structural resonances were pointed out. A comparison between the measured values and those suggested by the German Code was also done.
An interesting solution used to preserve a sixteen century building in Rome is also discussed.

## 2. EXPERIMENTAL INVESTIGATION AND DATA ANALYSIS

Seismometers and displacement trasducers were located in different time on each monument. The signals were recorded on magnetic tape by an analog recorder and then digitized with a high frequency sampling rate (0.005 sec). For each structure several registrations at different hours of the day and in different days were carried out.
Intervals of 30 minutes length of all the records were analyzed performing statistical and spectral analyses. The statistical analysis consisted in the calculation of the effective values and the peak values of the velocity over successive intervals lasting 1.28 seconds. The effective values were calculated using the formula

$$x_{ef} = \sqrt{\frac{\int_{t_1}^{t_n} x^2 dt}{t_n - t_1}}$$

where $x$ is the recorded value and $t_n$-$t_1$ the time interval. In more detail, for each seismometer the positive, negative and absolute peak values were pointed out and the effective their maximum, minimum and average values with standard deviation were calculated.
In Tab. 1 are summarized the maximum values of the effective and peak values of the velocity on the basement and at the top of each monument.
For each monument the frequency domain analysis was carried out plotting the power spectral density for each record and the cross spectral density with the phase factor between a reference record and each of the other ones [3, 4, 5]. The coherence function was also calculated. Spectral analysis allowed to individualize the structural resonances and the first modal shapes on the basis of the spectral amplifications [1, 6].

## 3. TRAFFIC INDUCED VIBRATIONS EFFECTS

Almost all the velocity diagrams recorded at the basement of the monuments are characterized by a ground noise and intervals of higher vibrations. The ground noise is related to ambient vibrations and to the vehicular traffic. Vibrations of higher amplitude are due to the passing of the train. In fact, most of the considered monuments in Rome are near the underground. The amplitude of the vibrations during the passing of the train are four-five times higher than those relative only to the ground noise.

In Figs. 1 and 2 are plotted the records of the sensors located in the same horizontal direction, respectively on the basement and at the top of the Arco di Costantino. Figs. 3 and 4 show the diagrams of the effective velocities and Figs. 5 and 6 the diagrams of the peak values of the same records.

| | Basement | | Top | |
|---|---|---|---|---|
| Monument | Effective values | Peak values | Effective values | Peak values |
| Arco di Costantino | 0.097 | 0.340 | 0.210 | 0.283 |
| Tempio della Minerva Medica | 0.115 | 0.379 | 0.711 | 2.210 |
| Colonna Antonina | 0.026 | 0.064 | 0.130 | 0.284 |
| Colonna Traiana | 0.033 | 0.094 | 0.340 | 0.478 |
| Anfiteatro Flavio | 0.122 | 0.155 | 0.121 | 0.325 |
| Trofei di Mario | 0.072 | 0.128 | 0.069 | 0.245 |
| Terme di Caracalla | 0.032 | 0.075 | 0.164 | 0.395 |

Tab. 1 Maximum effective and peak values of the velocity (mm/s) on the basement and at the top of the monuments

The maximum values were compared with that suggested as the limit value of the velocity at the basement of historical constructions by German Code DIN 4150. This being equal to 2-3 mm/s, we can conlcude that the velocities of the traffic induced vibrations on the monuments in Rome are very low. Therefore they do not represent an immediate hazard to historical constructions.

In spite of that traffic induced vibrations may be very dangerous. It depends on the mechanical characteristics of the monument and on its structural state.

| Monument | Effective values | Peak values |
|---|---|---|
| Arco di Costantino | 2.16 | 0.93 |
| Tempio della Minerva Medica | 6.18 | 5.83 |
| Colonna Antonina | 5.00 | 4.44 |
| Colonna Traiana | 10.3 | 5.08 |
| Anfiteatro Flavio | 1.00 | 2.10 |
| Trofei di Mario | 0.96 | 1.91 |
| Terme di Caracalla | 5.12 | 5.27 |

Tab. 2 Ratios between the values at the top and on the basement of the maximum effective and peak velocities

In Tab. 2 are reported the ratios between the maximum effective values and the peak values recorded at the top and those recorded on the basement of each monument. As we can see the values are very scattered.

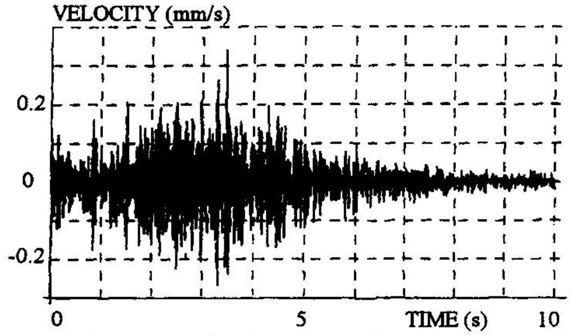


Fig. 1 Velocity on the basement (Arco di Costantino)

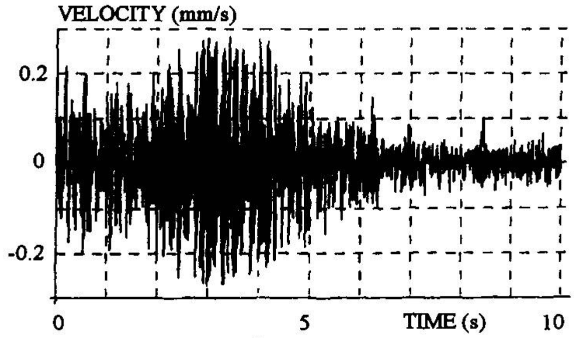


Fig. 2 Velocity at the top (Arco di Costantino)

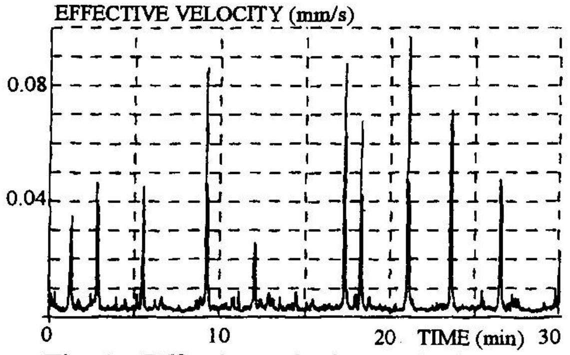


Fig. 3 Effective velocity on the basement

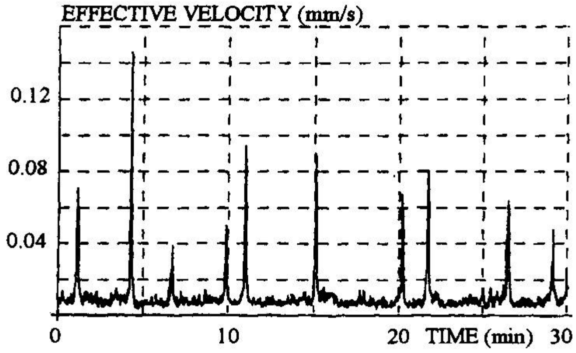


Fig. 4 Effective velocity at the top

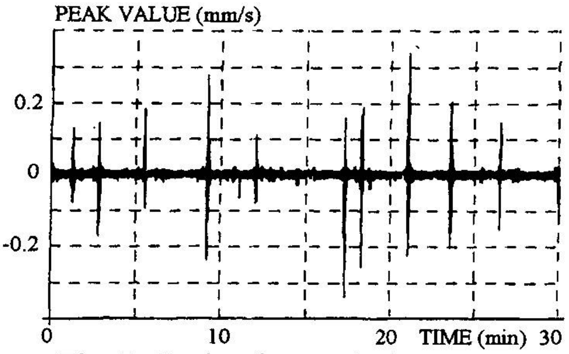


Fig. 5 Peak value on the basement

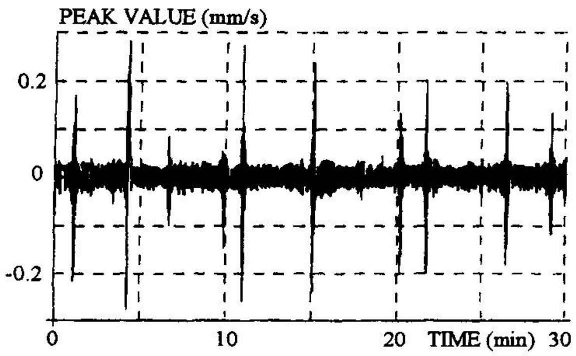


Fig. 6 Peak value at the top

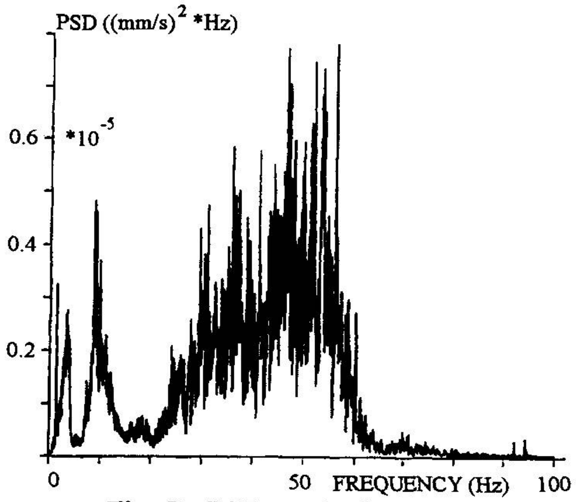


Fig. 7 PSD on the basement

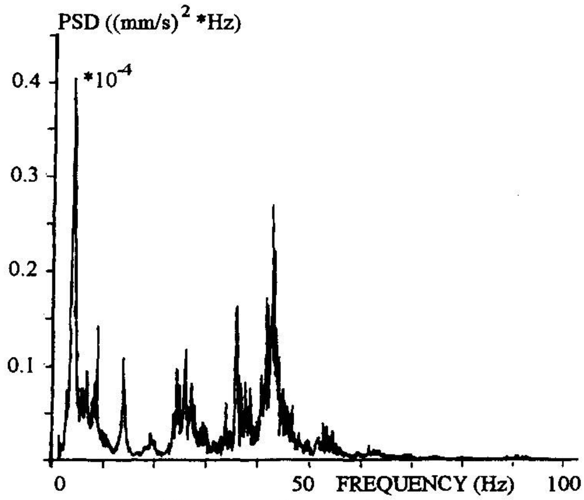


Fig. 8 PSD at the top

In some cases the difference between the effective velocities at the top and the basement is very low. Particularly vulnerable is the Tempio della Minerva Medica, for which the absolute peak value of the velocity at the top is very high (>2 mm/s). This monuments lies quite near to Termini Station (the main station in Rome) and another secondary railway runs just next to it.
The frequency content of the traffic induced vibrations is very wide, as we can see from the power spectral density of the signal recorded at the basement of the Arco di Costantino (Fig. 7). The power spectral density of the signal at the top of the monument is quite different (Fig. 8). In the first case high frequencies components are present in the signal, in the second one the peak at lower frequencies are more evident. This is obviously due to the filtering of the structure.

## 4. A CONTROL SYSTEM OF TRAFFIC INDUCED VIBRATIONS

To preserve a structure from the traffic induced vibrations an isolating system can be used. This kind of vibration control system is often adopted for the new constructions in seismic area. It is not very suitable in the case of existing structures.
An interesting solution was proposed by Colonnetti at the end of 50's to preserve Villa Farnesina, a building of the beginning of the sixteen century, from the effects of the heavy traffic [8]. The cartroad and not the building was isolated from the ground. The structure of the road was modified in order to peak up the wawes on their way to the soil under the road. This kind of solution offers the advantage to be effective for a large area including several constructions. For this reason it is very suitable for the central areas of the ancient cities.
In more detail, a rigid prestressed concrete gridwork on elastic rubber supports was built. The rubber supports were placed on a concrete slab laying on the road-bed. Concrete plates were placed on the grid and, over them, the bitumen paving.
The intervention, completed in 1970, interested a portion of the road of 64.52 m length, with a depth of 1.65 m. 1000 rubber supports were used, whose size was 22*12*3 (cm). Tipical bridge joints were utilized at the ends of the grid. The cost of the intervention was 50000 Italian Lire per square meter. According to the designer this solution guaranteed a reduction of the vibration amplitude of 80%.

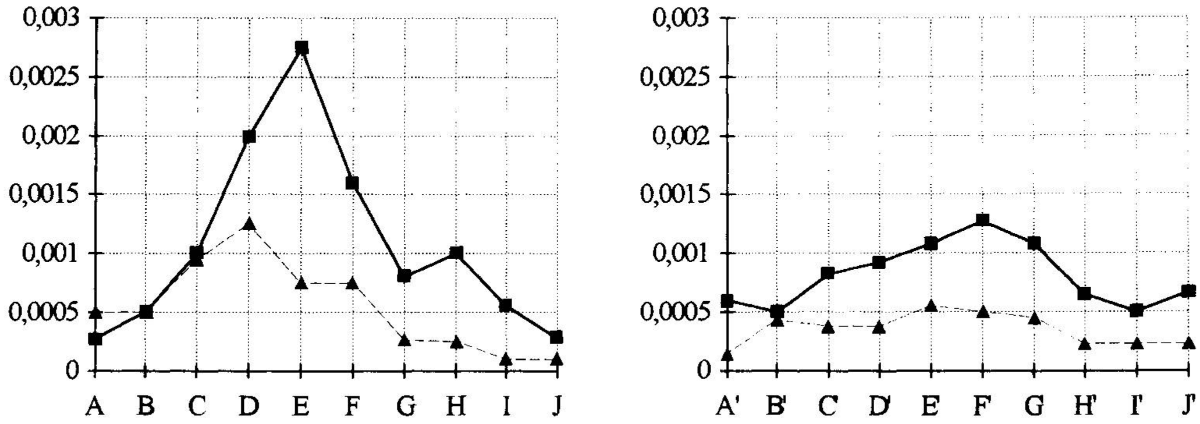


Fig. 9 Peak values of the ratio *a/g* recorded under and on the basement of Villa Farnesina

In Fig. 9 are shown the results of the drop impact tests carried out before the intervention in order to find the maximum amplitudes of the acceleration under the basement (triangles) and on the ground floor (squares) of the building and the zone on the road of maximum disturbance [8]. A to J were the position in which a mass of 70 Kg were dropped along the road on the pavement at the same side of the building. A' to J' were the corresponding locations on the other side of the road.

The distance between the first point A and the last one J was about 200 m. The drop impact tests simulated very well the effects due to the impact of a lorry weel in the holes in the cart-road.
This was the first time, in Europe and in the world, that a road was repared to preserve a monument from the traffic induced vibrations. A similar solution had already been used in Rome to preserve the Terme di Diocleziano from the vibrations induced by the traffic of the new Via Parigi [8].

## 5. CONCLUSIONS

Nowadays the effects due to the vehicular traffic are limited, because of the good quality of the pavings. Therefore our attention is focused on the effects of the vibrations induced by the passing of the trains. These can be very dangerous for structures already damaged and for old masonry structures. In fact, vibrations of small amplitude but characterized by a high number of cycles cause the reduction of the masonry strength due to the deterioration of the mortar and to its detachment from the bricks. Particularly vulnerable are the monumental buildings, bacause of the poor mortar used to build them.
The solution adopted for Villa Farnesina seams to be very interesting in the cases in which the railway is quite near to the structure and the vibrations induced by the trains are very dangerous, as in the case of the Tempio della Minerva Medica.
Anyway the monitoring of the construction is advisable in order to study the traffic induced vibrations in every specific case.

## REFERENCES


1. BENDAT J.S., PIERSOL A.G., *Engineering application of correlation and spectral analysis*, John Wiley and Sons, 1980.
2. BONGIOVANNI G., CELEBI M., CLEMENTE P., The Flaminio Obelisk in Rome: vibrational characteristics as part of preservation efforts, *Earthquake Engineering and Structural Dynamics*, Vol. 19, No. 1, 1990.
3. CLEMENTE P., BONGIOVANNI G., Ambient Vibration Effects on the Colosseum, *Proc. IABSE Symposium "Structural Preservation of the Architectural Heritage"*, Rome, 1993.
4. CLEMENTE P., BONGIOVANNI G., MARZI C., La colonna Antonina in Roma: valutazione degli effetti delle vibrazioni ambientali, *Proc. 3rd Italian Workshop ASS.I.R.C.CO.*, Catania, 1988.
5. CLEMENTE P., RINALDIS D., BONGIOVANNI G., Dynamic characterization of the Tempio della Minerva Medica, *Proc. 10th European Conference on Earthquake Eng.*, Vienna, 1994.
6. EWINS D.J., *Modal testing: theory and practice*, Research Study Press, 1984.
7. ISMES, *Rilievo di vibrazioni indotte dal traffico metropolitano e/o autoveicolare su monumenti antichi della citta di Roma*, Report to ENEA, 1985.
8. RINALDIS D., CLEMENTE P., DONZELLI R., Analisi e controllo delle vibrazioni della Farnesina, *Proc. Workshop "Terremoti in Italia: previsione e prevenzione"*, Accademia Nazionale dei Lincei, Rome, 1994.

# Field Measurement of a Steel Railway Bridge with Rubber Bearings

Mesures sur des ponts ferroviaires métalliques avec appuis en caoutchouc

Vermessungen einer Stahleisenbahnbrücke mit Gummilagern

**Kenichi YAGINUMA**
Civil Engineer
East Japan Railway Company
Tokyo, Japan

**Yoshio TAKAGI**
Deputy Manager
East Japan Railway Company
Tokyo, Japan

**SUMMARY**

There are many instances of metallic bearings used in steel railway bridges being deformed. The authors want to make use of the advantage of rubber bearings which reduce the load imposed on the top of an abutment or a pier. This paper reports on the results of measurement of a steel railway bridge with rubber bearings under a long-term use.

**RÉSUMÉ**

De nombreux cas de déformation d'appuis métalliques sont constatés dans les ponts ferroviaires métalliques. Les auteurs veulent profiter des avantages d'appuis en caoutchouc qui exercent moins de charge sur la tête de la culée ou de la pile. L'article décrit le résultat de mesures effectuées pendant une longue période sur des appuis en caoutchouc de ponts ferroviaires.

**ZUSAMMENFASSUNG**

Es gibt viele Schäden an den Stahllagern von Eisenbahnbrücken, die sich deformieren. Die Autoren wollen deshalb den Vorteil von Gummilagern nutzen, weil das Gummilager die Lageroberfläche weniger belastet. Es wird berichtet über die Messresultate einer Eisenbahnbrücke aus Stahl mit Gummilagern nach Langzeitgebrauch.

## 1. INTRODUCTION

We carried out a measurement at the support to Tokyo (the fixed side), of Minami-Senju Anti-Overflow Bridge (Overbridge) on Joban-Up Line described in Document [1] , as a follow-up survey. This bridge is a deck plate girder, measuring 6m span length, for about 10 years in service. The rubber bearings have been laid was erected, but the sole plate is not set up especially. The measured position is shown in Figure 1 and the content of the measurement at each point of measurement is shown in Table 1.

Moreover the fatigue test of rubber bearings prior to the application to the bridge was carried out. Rubber bearrings' fatigue due to the horizontal shearing deformation and the vertical deformation under 2,000,000 cycles of loading was investigated under the condition assumed to occur when they were used for the steel railway bridge. The rubber bearings are judged to be fit for practical use in terms of the support and the fatigue durability performance from this examination result.

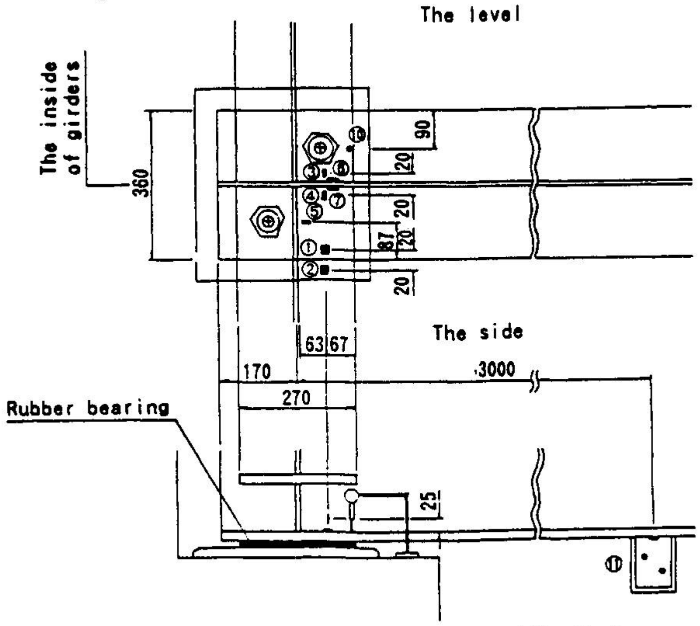


Figure 1 Measurement position (①-⑪ in figure corresponds to No. in Table 1)

Table 1 Content of measurement

| No | Sort of gauge etc. | Measured position | Measured items |
|---|---|---|---|
| ① | accelerometer (10G) | on the lower flange at the support in a main girder | characteristic of vibration |
| ② | accelerometer (5G) | on the top mortar of an abutment | characteristic of vibration |
| ③ | gauge of single axis | on the lower flange at the support in a main girder (the right angle direction to a main girder, the inside of girders) | local stress |
| ④ | gauge of single axis | on the lower flange at the support in a main girder (the right angle direction to a main girder, the outside of girders) | local stress |
| ⑤ | gauge of single axis | on the lower flange at the support in a main girder (the direction of a main girder, the outside of girders) | local stress |
| ⑥ | gauge of single axis | at bottom of the web at the support in a main girder (the inside of girders) | local stress |
| ⑦ | gauge of single axis | at bottom of the web at the support in a main girder (the outside of girders) | local stress |
| ⑩ | dial gauge | on the lower flange at the support in a main girder | train's running stability and riding comfort under deflection |
| ⑪ | non-contact displacement gauge | the deflection of a main girder at the span center | train's running stability and riding comfort under subsidence |

## 2. RUBBER BEARING'S STRUCTURE AND MATERIALS

The rubber bearing which is used in a steel railway bridge has stainless steel plates on both faces of chloroprene rubber 8mm-16mm thick. The number of heavy layers of rubber bearings is three.
Moreover, rubber used for the rubber bearing is high-quality chloroprene rubber which excels in the low temperature characteristic and meeting the standard shown in Table 2 of C08-b1 of JIS K 6386 (Rubber Materials for Vibration Isolators).

Table 2 Rubber's quality standard

| Physical characteristic | | Unit | Standard value |
|---|---|---|---|
| static shear modulus of rigidity | | kgf/cm² | 8±1.0 |
| hardness | | | 50±5 |
| elongation | | % | over 400 |
| oil resistivity (transition modulus of volume) | | % | under +120 |
| aging resistivity | transition modulus of 25% elongation stress | % | -10-+100 |
| | transition modulus of elongation | % | over -50 |
| strain modulus of compression permanence | | % | under 35 |
| ozone resistivity | | | no crack to the naked eye's observation |
| coldness resistivity | | ℃ | under -40 |

## 3. THE EQUIPMENT USED FOR THIS MEASUREMENT AND ANALYSIS

A bridge diagnosis system (BMC system) was used in the measurement and the analysis. This system is the one that integrates the bridge's maintenance which was implemented in the field by practiced inspectors so far. It is devised to operate easily, and has the function to do another real bridge measurement, its soundness diagnosis, and various analyses concerning the structure efficiently.
Moreover a non-contact displacement gauge was used for the measurement of the deflection of the span center of a main girder. This has the characteristic to be able to measure a bridge even over the road where traffic is heavy and the river, and able to measure the roll besides the deflection, unlike the old ring type deflectometer.

## 4. RESULTS OF EXAMINATION

### 4.1 The Effect of Reducing Vibration at a Support

#### 4.1.1 Examination by Accelerations

The decrease degree of a vertical acceleration on the lower flange at the support in a main girder and on the top mortar of an abutment was investigated. The measuring trains are No.1-No.7 of Table 3 and an acceleration wave form of train No.6 is illustrated in Figure 2 and Figure 3. The peak appears at several places, and we think this is the influence of impact of wheel flats and the like. Table 4 shows the comparison between the measured results of this examination and Document [1]. It can be said that the anti-vibration effect is evident th ough there are some variations in the maximum vertical acceleration and in the decrease degree of the acceleration on the lower flange at the support in a main girder and on the top mortar of an abutment.

#### 4.1.2 Frequency Analysis

The shape of vertical acceleration waves were spectrum-analyzed (Fourier-transformed) and frequency-analyzed by the BMC system. The case of train No.6 is shown as one example. Figure 4 shows frequency analysis of a vertical acceleration on the lower flange at the support in a main girder. The power spectral density is generally high at each frequency and the dominant frequency does not appear clearly. On the other hand, Figure 5 shows frequency analysis of a vertical acceleration on the top mortar of an abutment. The dominant frequency appears remarkably and power spectral densities of other frequencies are values closest to 0. As a result, it is understood that the frequency elements other than the dominant frequency have been cut through the rubber bearing when the vibration is transmitted from the lower flange to the top of an abutment. It can be said from the thing that the effect of reducing the vibration is evident.
The dominant frequency at the support happened to be different in the values by trains, being 30Hz-77Hz. These values are alm ost the same values on the lower flange and on the top of an abutment.

Table 3 Measuring trains

| No | Sort of train | the number of cars | speed (km/h) |
|---|---|---|---|
| 1 | local electric train | 10 | 53 |
| 2 | limited express electric train | 7 | 55 |
| 3 | limited express electric train | 11 | 62 |
| 4 | local electric train | 7 | 44 |
| 5 | local electric train | 10 | 51 |
| 6 | limited express electric train | 7 | 55 |
| 7 | limited express electric train | 11 | 75 |
| 8 | local electric train | 10 | 30 |
| 9 | local electric train | 10 | 30 |
| 10 | local electric train | 11 | 22 |
| 11 | local electric train | 15 | 38 |
| 12 | limited express electric train | 11 | 39 |
| 13 | local electric train | 10 | 32 |
| 14 | limited express electric train | 7 | 62 |

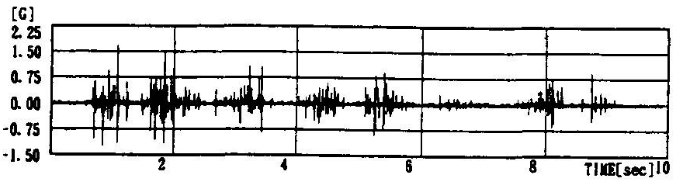


Figure 2 The wave forms of vertical acceleration on the lower flange at the support

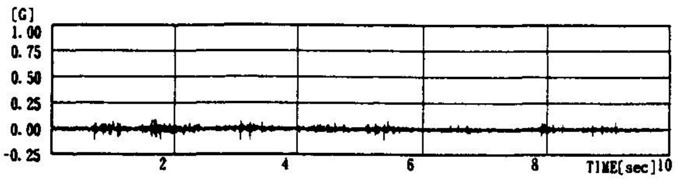


Figure 3 The wave forms of vertical acceleration on the top mortar of an abutment

### 4.2 The Evaluation of Train's Running Stability and Riding Comfort

Because the deflection of a girder, the unevenness, etc., have been taken as indexes of train's running stability and riding comfort so far, the evaluations were done hereaccording to these indexes, too.

#### 4.2.1 The Deflection at the Span Center

Table 4 Measured result (acceleration)

| Category | This examination (7 trains) | Document[1] (4trains) |
|---|---|---|
| the maximum vertical acceleration on the lower flange at the support in a main girder | 0.3G-1.8G | 0.7G-2.7G |
| the maximum vertical acceleration on the top mortar of an abutment | 0.04G-0.2G | 0.10G-0.2G |
| the decrease degree of the acceleration | 7.5G-17.0G | 6.6G-22.4G |

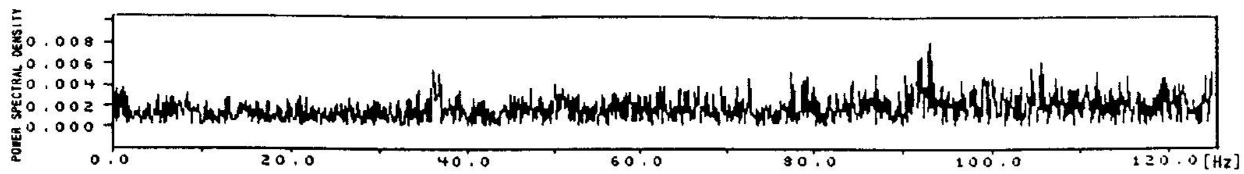

Figure 4 Frequency analysis of vertical acceleration on the lower flange at the support

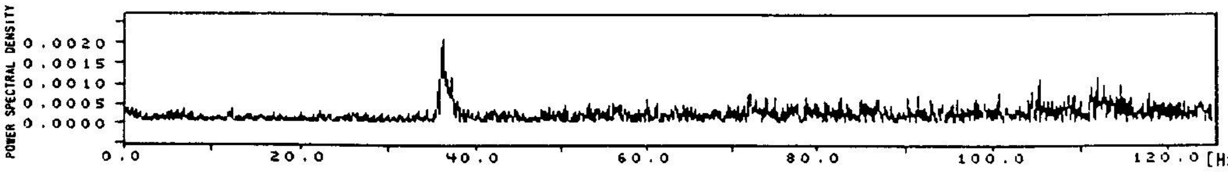

Figure 5 Frequency analysis of vertical acceleration on the top mortar of an abutment

Measuring trains for the deflection of a main girder at the span center are four (No.10 and No.12-No.14 of Table 3), and the measured result including Document [1] is shown in Table 5. Both can be said to differ little. The wave forms by train No.14 are shown in Figure 6 as one example. Moreover, because the values contain the subsidence and the impact value at the support due to rubber bearing's elastic deformation, and moreover, they are far smaller than deflection's limit value L/800 of a main girder, there will be no problem.

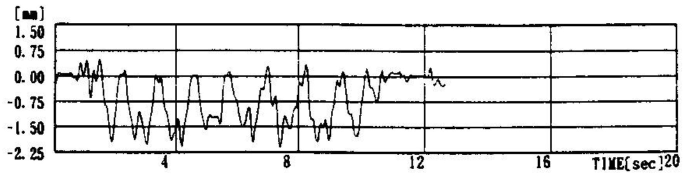

Figure 6 The wave forms of deflection at the span center

### 4.2.2 The Vertical Unevenness at The Support

The subsidence shown in Table 5 was caused at a support in a main girder (the case of train No.14 is shown in Figure 7 as an example of the wave form). Because the value is much smaller than deflection's limit value 4mm at a crossing both at an end floor beam and an end stringer laid down empirically as the index of train's running stability and riding comfort, when a train goes from an abutment into a bridge and goes out of it, this is not a value nothing any problem, either.

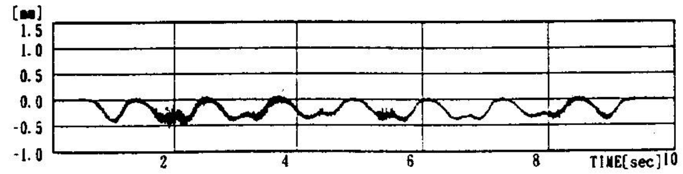

Figure 7 The wave forms of subsidence at a support

Table 5 Measured result (deflection and subsidence)

| Category | This examination (4 trains) | Document[1] (4trains) |
|---|---|---|
| the deflection of a main girder at the span center | 2.0mm-2.6mm | 1.9mm-3.0mm |
| the subsidence at a support in a main girder | 0.3mm-0.6mm | ———— |

## 4.3 The Evaluation of Local Stress and Fatigue at a Support

### 4.3.1 Local Stress at a Support

Measuring trains to examine the local stress of the support were seven, that is, No.8-No.14 of Tables 3. Being local stresses, the maximum amplitude stresses were as small as 10MPa-25MPa though wave forms were different by measured points.

#### 4.3.2 Evaluation by Fatigue Damage Degere

Fatigue damage degree at bottom of web plate at a support was calculated by BMC system. Here the fatigue damage degree is the fatigue degree when one train has passed, and when the accumulation reaches 1, fatigue damage will be caused to the joint concerned. The stress range which had been used to calculate was assumed to be the stress range generated in the direction of steel plate surface whose value was larger than the bending stress range generated in the right angle direction to steel plate surface (it was calculated from strain gauge of single axis pasted to inside and outside across web plate by BMC system). The welded joint at the bottom of web was assumed that 2000000 cycles basic allowable fatigue stress range was $\Delta\sigma_{f0}$=80MPa (there was full penetration welded joint at bottom of the web, and the fillet welded joint of the load-non-transmitted and non-finish type was assumed). In one example of measurement by train No.14, fatgue damage degree was $D_0$=0.023*$10^{-6}$, which means that the first fatigue damage to the welded joint at the bottom of lower flange comes after about 40,000,000 times of the train passage. Therefore it is understood that there is considerable reserve of strength.

#### 4.3.3 Revision of Sole Plate Standard Thickness

Accordingly, it has been understood that there are not any problems concerning the local stress, at the support even when there is no sole plate like this bridge. However, because reaction in the support may not be distributed easily and equally, and dust may collect easily with possible corrosion, and so on, in the vicinity of a bearing, it is decided to revise the standard such that the sole plate is set more than 22 mm in thickness as in the case of general bearings. In general, the sole plate is more often set 28 mm in thickness because the plate is gouged and it is fastened with high strength bolts.

## 5. CONCLUSIONS

To sum up to results :

(1) As a result of measuring the vibration of the support, it has been understood that the effect of reducing the vibration is retained as well as immediately after this bridge was erected. The same can be said from the frequency analysis result.

(2) As a result of examination, it has been understood that running stability and riding comfort are retained as good as immediately after the bridge was erected, with no problem about the value obtained.

(3) Because, in this bridge which did not use the sole plate, it has been understood that there is no problem about the local stress and fatigue at the support, the sole plate thickness is held same as in general bearings. Moreover, the standard is revised to specify hot dip galvanizings of zinc as anti-rust protection of the sole plate.

According to the result, rubber bearing's utility, and especially its performance sometime after being erected, was able to be confirmed. Future policy will be to adopt the rubber bearing for a steel railway bridge more aggressively than before.

## ACKNOWLEDGMENT

The writers wish to thank the staff of Bridge Laboratory, Railway Technical Research Institute, and in BMC, Inc. for the measurement and analysis they have done.

## REFERENCE DOCUMENTS

[1] Ichikawa, A., Taketomo, N. : Examination of Rubber Bearings for a Steel Girder, Structural Designing Data, No.75, 1983 (in Japanese).

# Dynamic Load Testing of Swiss Bridges

## Essais dynamiques des ponts en Suisse

## Dynamische Versuche an Schweizer Brücken


**Olivier L. BURDET**
Dr. Eng.
Swiss Fed. Inst. of Technology
Lausanne, Switzerland

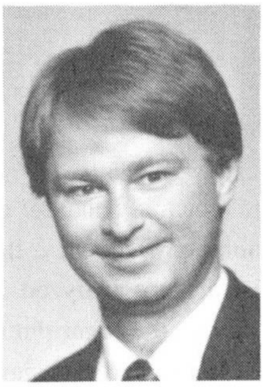

Olivier Burdet, born in 1960, holds a Ph.D. from the University of Texas at Austin. He is in charge of field testing for IBAP and also involved in teaching and research activities. His research interests include bridge evaluation and maintenance and design by testing.

**Stéphane CORTHAY**
Assistant
Swiss Fed. Inst. of Technology
Lausanne, Switzerland

Stéphane Corthay, born in 1967, holds a Civil Engineering degree from EPFL. He is involved in static and dynamic load testing of bridges.



**SUMMARY**

The paper presents results obtained using a simple dynamic testing procedure frequently used in Switzerland for highway bridges. Typical results are shown and tendencies observed in the dynamic behaviour of highway bridges are presented. For a deteriorated pavement, the dynamic impact of heavy vehicles is shown to be larger at lower truck speeds. Some correlation is shown between the dynamic properties of the bridge and its stiffness, as measured in a static load test.

**RÉSUMÉ**

L'article présente les résultats obtenus à l'aide d'une méthode d'essai dynamique simple fréquemment utilisée pour les ponts routiers en Suisse. Le comportement typique des ouvrages, ainsi que les tendances générales des ponts routiers sont présentés. Dans le cas d'un revêtement détérioré, il est montré que le coefficient d'amplification dynamique est plus grand lorsque la vitesse de passage des véhicules est plus faible. Quelques corrélations sont présentées entre les propriétés statiques et dynamiques des ponts.

**ZUSAMMENFASSUNG**

Im vorliegenden Bericht werden die Ergebnisse einer einfachen Testprozedur für dynamische Belastungsversuche präsentiert, die in der Schweiz oft für Brücken verwendet wird. Typische Versuchsergebnisse und Tendenzen der Autobahnbrücken werden gezeigt. Bei beschädigter Fahrbahnfläche ist der dynamische Amplifikationsfaktor schwerer Fahrzeuge bei kleineren Fahrgeschwindigkeiten oft grösser. Gewisse Korrelationen zwischen den statischen und dynamischen Brückeneigenschaften werden aufgezeigt.

## 1. Introduction

Dynamic load testing is an important part of the acceptance process for new bridges in Switzerland [8]. As a complement to static load tests, dynamic tests yield useful information about the actual behavior of the bridge under traffic. This information is usually difficult to obtain analytically, because of the complexity of the actual structure. The effect of pavement deterioration on the dynamic response of the bridge is of particular importance for the management of the structure. This information can be easily and realistically obtained from a dynamic test, and thereafter used by the highway authorities to organize the pavement maintenance.

Drawing on the large number of tests performed by IBAP over the past twenty years, the paper describes the general dynamic characteristics of highway bridges. Some correlation is shown between the stiffness obtained in a static load test and the measured eigenfrequencies. The influence of the speed of a vehicle crossing the bridge is discussed. In particular, the effect of an artificial damage in the pavement on the dynamic behavior is presented.

## 2. Dynamic Load Testing

The purpose of the dynamic load test is to determine the controlling parameters of the dynamic behavior of the bridges. The main dynamic characteristics of the structure are the fundamental vibration frequency, the dynamic amplification factor and the logarithmic decrement. These properties are usually not analyzed in detail in the design phase of small and middle sized structures. Some parameters, such as the logarithmic decrement or the dynamic amplification factor, can only be roughly estimated at the time of the design. However, these quantities are relatively easy to obtain experimentally, and can give valuable information for the exploitation and maintenance of the bridge.

The general methodology used in the dynamic load test of a bridge will be presented using as an example the bridge shown in figure 1. The Riddes-Leytron bridge is a cable-stayed structure with a slender deck, supporting two lanes of traffic and a sidewalk. The bridge was built from 1991 to 1992 and tested in the summer of 1992.

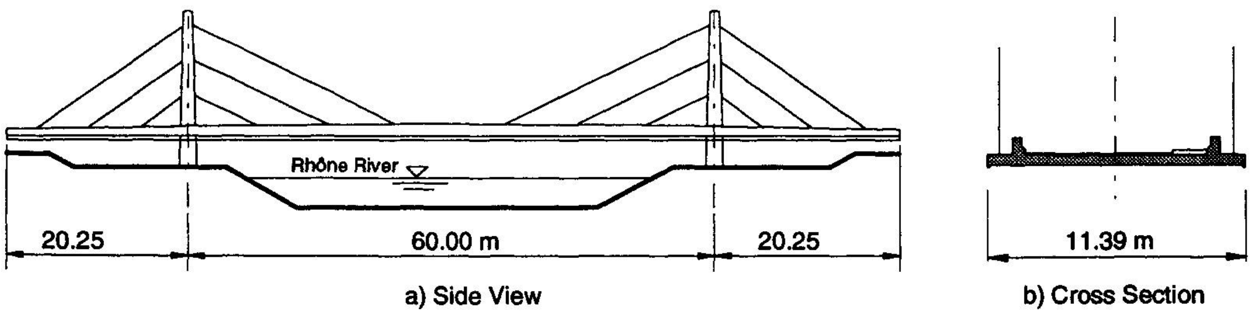


Figure 1: Geometry of the Riddes-Leytron bridge

## 3. Methodology

Dynamic load testing is performed by exciting the vibration of the bridge and by measuring its properties after the excitation has ceased. Several methods are available for the excitation of the bridge, in particular: eccentric rotating masses, impact of a heavy weight and passage of a loaded truck. This last method is often preferred for the dynamic load testing of bridges because it gives, along with reasonably accurate values of the above mentioned quantities, a good approximation of the effect of the actual traffic on the structure. By varying the speed of the truck on the bridge, the full range of traffic speeds can be investigated. Furthermore, this method is easily implemented while some of the other ones necessitate more complicated installation procedures. The measurements are taken and recorded by a dynamic data acquisition system with integrated Fast-Fourier Transform (FFT) analyzer, allowing an immediate interpretation of the results during the test.

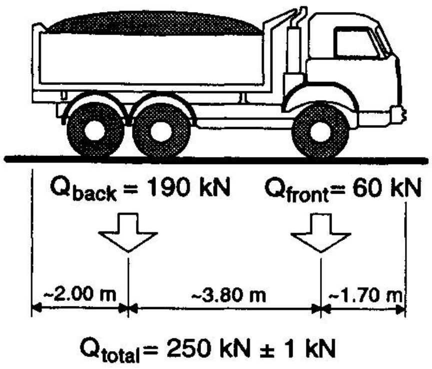


Figure 2: Typical truck used in dynamic load testing

The trucks used for the dynamic excitation of the bridge are usually 3-axle trucks, as shown in Figure 2, with a total weight of 250 kN (total mass of 25 metric tons), traveling on the bridge at several speeds. The effect of a deterioration of the pavement is simulated by the introduction of a normalized plank on the path of the truck. This induces a strong impact when the trucks passes at mid-span, that represents the effect of a pothole in the pavement, or the irregularity of the surface caused by packed snow. Figure 3 shows the location of the instruments and the results for the dynamic testing of the Riddes-Leytron bridge. Absolute displacement sensors are used for the measurements, and therefore only components with a relatively high frequency (larger than 0.2 Hz) are recorded, as shown in Figure 3a (vertical dispacement at mid-span as a function of the truck position). The static influence line of the truck passing on the bridge is then added to obtain the complete dynamic influence line shown in figure 3b.

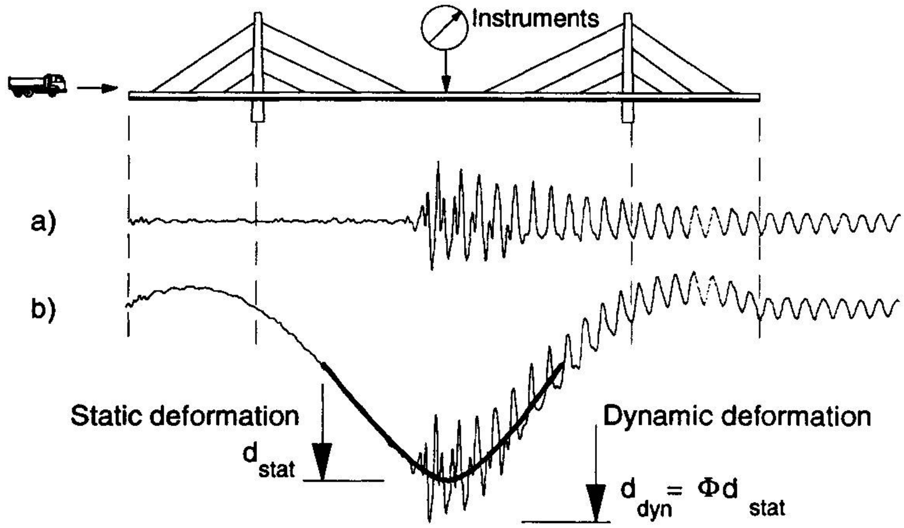


a) Relative vertical deflection at mid-span caused by the passage of the truck
b) Dynamic influence line of the passage of the truck. Determination of the dynamic amplification factor.

Figure 3: Description of the dynamic load test

## 4. Results

Because a lot of information is gathered in the course of dynamic load testing, the results are usually presented graphically. First, as shown in figure 3b, the dynamic influence line of the bridge subjected to the passage of a truck is drawn for all travel speeds, with and without plank. This allows a simple visual determination of the dynamic amplification factor $\Phi$. The natural frequency of the bridge is obtained from acceleration spectra performed by the FFT analyzer. The logarithmic decrement is obtained from the decay of the bridge free oscillations, after the truck has left the bridge, or at least when it is far enough from the instruments (figure 3a).

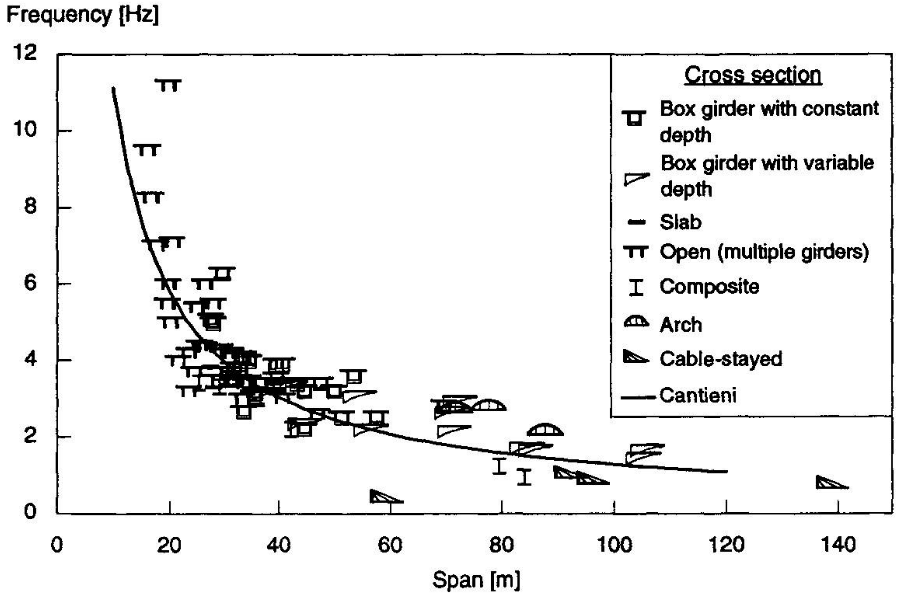


Figure 4: Natural frequency as a function of bridge span

Figure 4 shows the natural frequency as a function of bridge span for approximately ninety bridges tested by IBAP. The regression line was proposed by Cantieni in [5, 6], based on over 200 dynamic load tests of Swiss bridges. A good correlation has been found between his data and data gathered by IBAP. Figure 5 shows histograms of the dynamic amplification factor for the bridges tested over the past twenty years. Some bridges are not included in the graphs because of incomplete measurements in the early years of dynamic testing. The Swiss code for bridges specifies a constant dynamic amplification factor for bridges of 1.8. It is interesting to note that a significant number of bridges indicated higher values. Most bridges had a small damping, with logarithmic decrements smaller than 0.1.

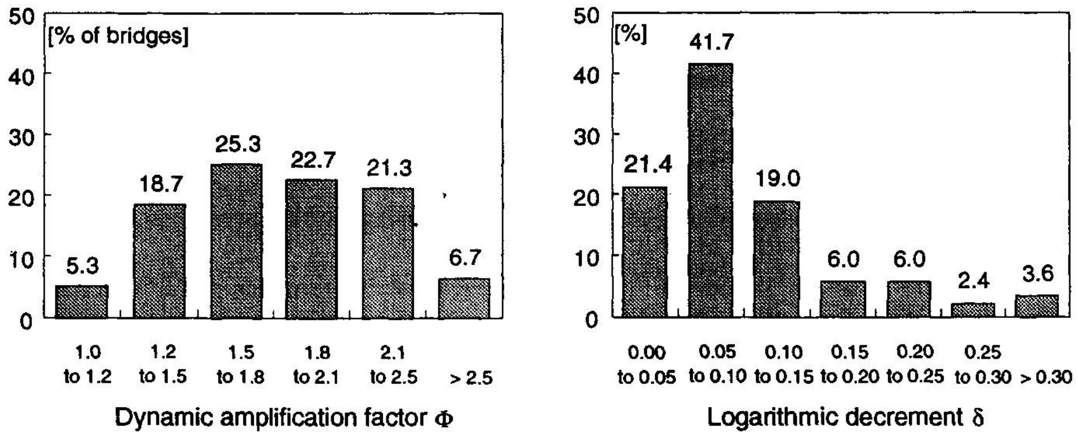


Figure 5: Histograms of the dynamic properties

Figure 6 shows the maximum measured vertical acceleration and displacement induced at mid-span of the Riddes-Leytron bridge by a passing truck, as a function of the truck speed. In the case of smooth riding surface, the response of the bridge is small and increases with increasing speed, while in the case of a deteriorated surface, the response is strong and the influence of the truck speed is less clear. It has been

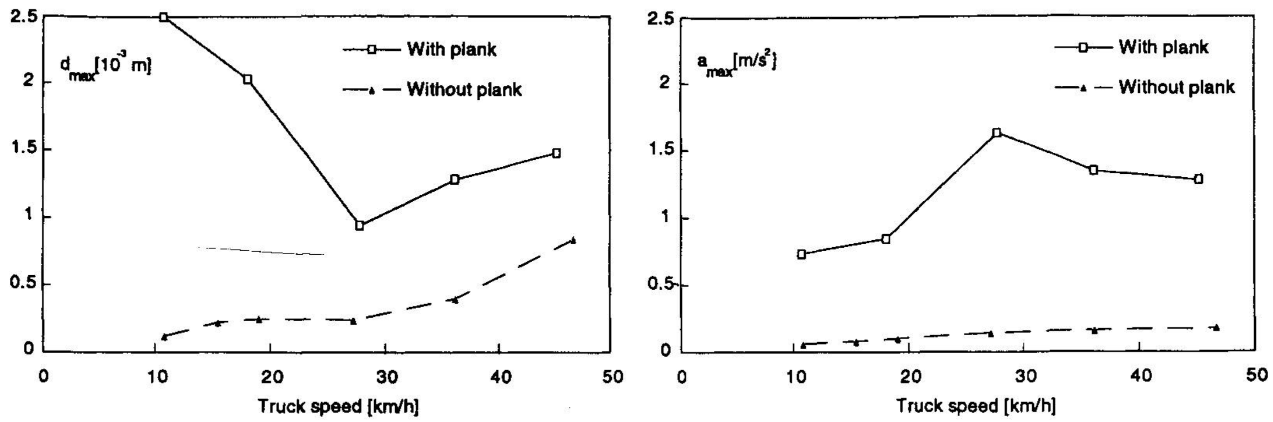


Figure 6: Dynamic response of the bridge as a function of the truck speed

observed in other structures that lower truck speeds can induce larger displacements (and accelerations) than higher speeds. One possible explanation is that a truck traveling at a lower speed will cause two distinct shocks as its two rear axles successively hit the plank. At low truck speeds, the two shocks occur approximately one second apart, which is close to the natural period of most bridges. At higher speeds, the two shocks are very close to one another, and remote from the natural frequency of the bridge

Human beings are especially sensitive to vibrations, particularly to accelerations. Some codes [2] give limiting values of acceleration as a function of the fundamental frequency. In practice, these limits are never reached if the riding surface is smooth, but they can be exceeded in the case of a deteriorated pavement. The results of the dynamic load tests give therefore useful information on the sensitivity of the bridge to deterioration, and can be used in defining the maintenance program for the pavement.

## 5. Comparison with the Results of Static Load Testing

Because dynamic loading testing is usually performed on bridges that have also been subjected to static load testing, comparisons can be made between the behavior of a bridge under static and dynamic loading. Clearly, the two behaviors are related, in that the bridge stiffness, or spring constant $k$ appears in both the static load test and in the components of the natural frequency. Figure 7 shows the fundamental frequency of

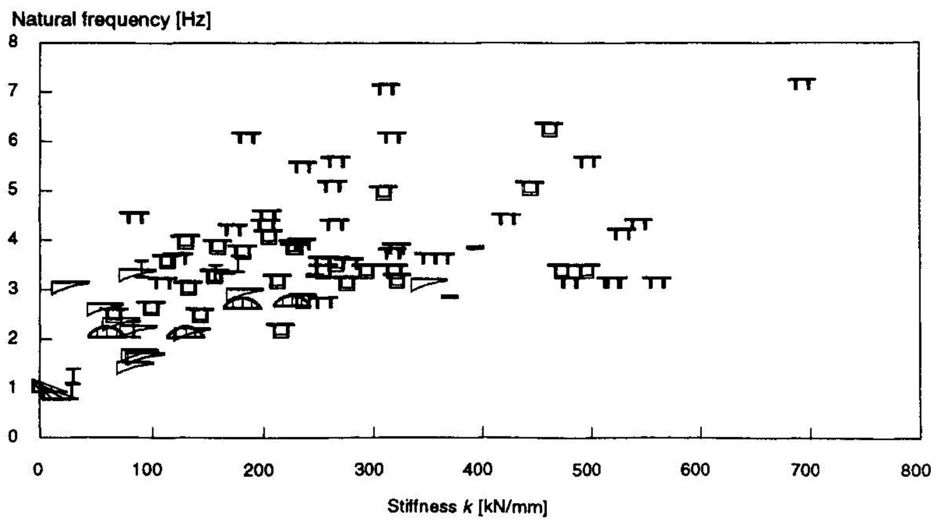


Figure 7: Natural frequency of the bridge as a function of the bridge stiffness

each of the tested bridges as a function of its stiffness obtained from a static load test. As expected, there is on average an increase in natural frequency with an increase in stiffness. However, the scatter is rather large, especially for concrete bridges, as their mass strongly depends on the construction method and cross section. A similar scatter can be observed when looking at the correlation between the dynamic amplification factor and the bridge span or natural frequency. While some tendencies can be observed, the scatter of the data makes the derivation of a simple approximate formula impractical.

## 6. Conclusions

The paper presents results obtained from simple dynamic load tests of bridges. These tests are frequently performed in Switzerland as part of the acceptance process of new bridges. The main results are the natural frequency of the bridge, the dynamic amplification factor and the logarithmic decrement.

By using a truck to induce vibrations of the bridge, it is possible to simulate the effects of pavement deterioration. Bridges that are especially sensitive to pavement deterioration are identified, and this information can then be used in establishing of the maintenance program of the structure. Truck speed is shown as having a great importance on the dynamic response of the bridge, especially in the case of a deteriorated riding surface.

Some correlation is shown between the span and the natural frequency of a bridge, but a considerable scatter is observed. In a similar manner, there is some correlation between the bridge stiffness observed in a static load test and the dynamic properties of the bridge.

## REFERENCES

[1] **HASSAN M., BURDET O.** and **FAVRE R.**, *Interpretation of 200 Load Tests of Swiss Bridges.* IABSE Colloquium: Remaining Structural Capacity, Copenhagen, Denmark, March **1993**.

[2] **NORME DIN 4150 (Teil 2)**, *Erschütterungen im Bauwesen, Einwirkungen auf Menschen in Gebäuden*, September 1975.

[3] **BURDET O.**, *Load Testing and Monitoring of Swiss Bridges*, CEB Informations Bulletin n° 219, August **1993**.

[4] **BURDET O., CORTHAY S.**, *Static and Dynamic Load Testing of Swiss Bridges*, International Bridge Conference, Warsaw, Poland, **1994**.

[5] **CANTIENI, R.**, *Dynamic Load Testing of Highway Bridges*, IABSE Proceedings, P-75/84, Zürich, August **1984**.

[6] **CANTIENI, R.**, *Dynamic Behavior of Highway Bridges Under the Passage of Heavy Vehicles*, Report no. 220, EMPA, Dübendorf, Switzerland, **1992**.

[7] **FAVRE R.**, *Risque de déformations irréversibles dans les ponts*, Journée OFR/GPC: Maintenance des ponts: résultats actuels de la recherche, Zürich, Switzerland, March **1993**.

[8] **SIA 169**, Recommandation, (Swiss Standard), *Recommandation pour la maintenance des ouvrages de génie civil* (Recommendation for the maintenance of Civil Engineering structures). Société suisse des ingénieurs et des architectes. Zurich, Switzerland, **1987**.

# Dynamic Characteristics of Port Mann Bridge by Modal Testing

Caractéristiques dynamiques du pont Port Mann à partir d'essais modaux

Dynamische Charakteristik der Port-Mann-Brücke, ermittelt durch modale Schwingungsmessungen

**Carlos E. VENTURA**
Assistant Professor
Univ. of British Columbia
Vancouver, BC, Canada

**Andreas J. FELBER**
President
EDI Ltd
Vancouver, BC, Canada

**Helmut G.L. PRION**
Assistant Professor
Univ. of British Columbia
Vancouver, BC, Canada

**Peter R. TAYLOR**
Vice President
Buckland & Taylor Ltd
Vancouver, BC, Canada

**Aegide VAN SELST**
Specialist
Buckland & Taylor Ltd
Vancouver, BC, Canada

## SUMMARY

This paper describes the vibration studies conducted at the Port Mann Bridge over the Fraser River, near Vancouver. Ambient vibration measurements were conducted on the 585 m long main span of the bridge and on one of the sections of its south approach. The information obtained from these tests was used to gain confidence in a computer model of the bridge used as part of a seismic assessment. The unusually light and flexible superstructure and the massive foundations presented an ideal opportunity to use ambient testing to increase understanding of prototype behaviour.

## RÉSUMÉ

Cet article présente les essais de vibrations effectués sur le pont Port Mann traversant la rivière Fraser près de Vancouver. Des mesures de vibrations furent effectuées sur la portée principale de 585 mètres du pont, ainsi que sur un des accès. L'information obtenue à partir de ces essais fut utilisée pour le calibrage d'un modèle de la structure utilisé pour une étude portant sur la sécurité parasismique du pont. Le faible poids et la flexibilité de la structure métallique par rapport aux fondations ainsi que les conditions du sol en place présentaient une occasion intéressante pour l'utilisation de mesures ambiantes afin de mieux connaître le comportement des prototypes.

## ZUSAMMENFASSUNG

Schwingungsstudien wurden an der Port-Mann-Brücke über den Fraser River nahe Vancouver durchgeführt. Verkehrs- und winderregte Schwingungen wurden an der 585 m langen Bogenbrücke und an der südlichen Anfahrtsrampe vorgenommen. Die ermittelten Schwingungsformen und Eigenfrequenzen wurden zur Verifikation eines Computermodells verwendet, welches zur Bestimmung der Erdbebensicherheit der Brücke diente. Die ungewöhnlich leichte und flexible Brücke bot eine ideale Gelegenheit für Schwingungsmessungen am bestehenden Tragwerk, was zu einem besseren Verständnis des dynamischen Verhaltens führte.

# 1. INTRODUCTION

The Port Mann Bridge , built in the early 1960s, is today a key component of the Trans Canada Highway carrying traffic across the Fraser River, between the municipalities of Coquitlam and Surrey, east of Vancouver, British Columbia, Canada. Because of the importance of the bridge and the seismic hazard of the region, in March of 1994 the Ministry of Transportation and Highways of British Columbia contracted Buckland and Taylor (B&T) Ltd. of Vancouver to assess the seismic behaviour of the bridge and to develop a seismic retrofit strategy. As part of this study, EDI Experimental Dynamic Investigations Ltd. was contracted to conduct a series of ambient vibration measurements of selected portions of the bridge. The tests were performed using the eight channel vibration measurement system of the University of British Columbia. Results from this study provided the necessary information to calibrate the analytical model of the bridge and its foundations used to determine its resistance to earthquake motions and to plan possible means of retrofit. This paper describes the results of the ambient vibration study (AVS) of the Main Span and a portion of the South Approach of the bridge, and the process followed to calibrate the computer model used in a three-dimensional dynamic analysis.

# 2. DESCRIPTION OF BRIDGE

A general overview of the Port Mann Bridge is shown in Fig.1. The bridge crossing is located where the Fraser River is about 900 m wide and consists of three structures: the Main Span and the North and South Approaches as shown in Fig.2. The Main Span crossing the navigational channel is formed by two three-span steel stiffened tied arches that provide a 44 m vertical clearance above high water level and a 365 m clear centre span for shipping. The side spans are 110 m long. The arches, in combination with the stiffening girders, were designed to act as a funicular polygon with no bending moments under dead load. The arch supports were pinned at pier N1, on longitudinal rollers at S1 and on rockers at N2 and S2, permitting longitudinal movement.

Because of poor foundation conditions, the weight of the superstructure was kept to a minimum. As a consequence, an orthotropic steel deck was chosen for the Main Span [3,4], which was designed to simultaneously fulfil the function of supporting the wheel loads and act as the upper flange of the stiffening girders. It also doubles as a horizontal diaphragm to transfer lateral loads and support the stiffening girder and arches. Longitudinal steel ribs are welded to the 12 mm thick

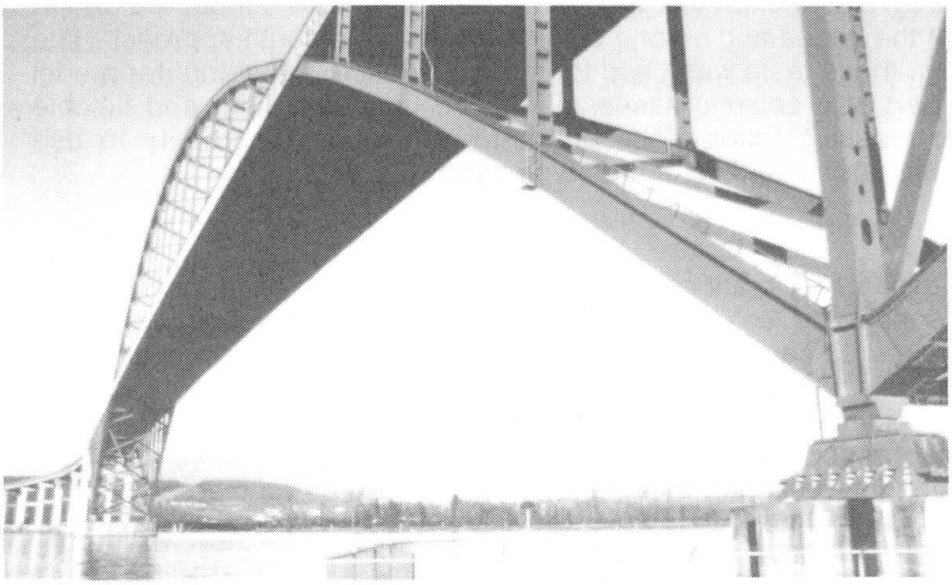

**Fig. 1** Underside View of the Port Mann Bridge

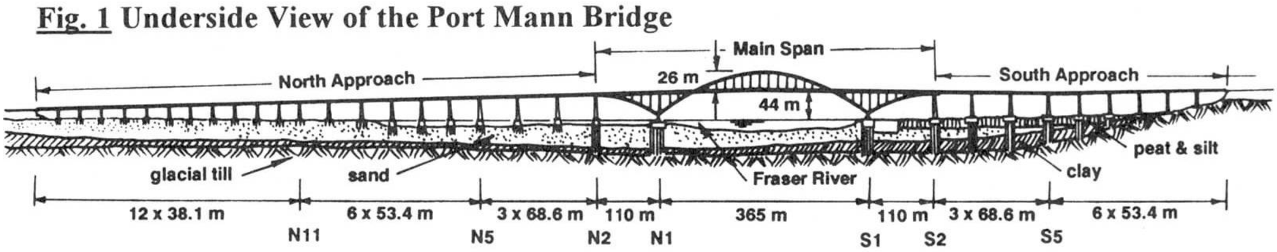


**Fig. 2** Elevation View of Port Mann Bridge

steel deck, forming panels 7.6 m long and spanning between the stiffening girders. A 50 mm layer of asphalt paving covers the steel deck. The 1.2 m wide sidewalks, made of precast lightweight concrete, are connected to the deck with stud welded anchor bolts. Cross beams that are tapered to provide the transverse roadway slopes, support the deck at 1.9 m spacing.

The arches consist of riveted steel boxes, 1.35 m deep and 1.32 m wide, with plate thickness varying between 27 mm at the apex and 38 mm at the supports. The stiffening girders are box sections with 12 mm thick webs, 3.66 m deep. The bottom flange consists of a 1.32m x 25 mm plate with 25 mm cover plates for local reinforcement; the top flange consist of a 1.48 m x 12 mm plate with one or two 20 mm cover plates over part of its length. The orthotropic deck forms part of the top flange.

Both hangers and columns are riveted I-sections built from medium grade angles and plates. All hangers except the shortest one have the same cross-section and have a slender appearance (533 mm deep). The cross-section of the columns below deck vary with length and have batten plates between the flanges. Cross braces at the main piers S1 and N1, and diagonal braces between the arches provide lateral stability to the structure. At the intersections of arches and stiffening girders, braces had to be eliminated to provide clearance for the traffic and a service gantry below. Boxed cross beams provide stiff portals to transfer the lateral loads across the openings.

The bridge approaches consist of a 200 mm thick reinforced concrete deck supported by three main steel plate girders and four stringers which are supported by cross beams at 5.7 m spacing. The North Approach consists of seven sets of three-span continuous composite girders with span lengths ranging from 38.1 m to 53.4 m to 68.6 m. The South Approach consists of three sets of three-span continuous girders with span lengths of 53.4 m and 68.6 m. The main girder depth varies from 1.68 m to 2.44 m to 3.36 m for the respective span lengths. The approach superstructure is supported on reinforced concrete bents with tapered hollow columns which are founded on common pile caps.

In general, the soil profile consists of compact till-like founding material at a depth of about 60 m, overlain by a 30 m layer of very sensitive marine deposited clay, topped by sand layers of varying density to within about 13 m of the surface. Along the south bank a thick layer of peat and silt overlays the sand. The thickness of the clay decreases and the sand layer increases towards the north side of the river. The four piers supporting the Main Span (S2, S1, N1 and N2) and the South Approach bents S3, S4 and S5 have the most problematic foundations and rely on a total of 612 concrete-filled steel tubular piles, some in excess of 65 m deep. The main piers S1 (which is D-shaped and located on the south bank) and N1 (which has an elliptical shape) are aligned along the flow direction of the river, resulting in a skewness of 27 and 16 degrees with respect to the bearing lines respectively.

As a reference, the mass of the superstructure is about $16*10^6$ kg while the masses of the main piers are about $20*10^6$ kg (N1) and $23*10^6$ kg (S1). Details of the foundations and soil conditions determined at the time of construction of the bridge are given by Golder and Willeumier [2].

## 3. VIBRATION MEASUREMENTS

The AVS was conducted in two phases. The work during the first phase concentrated on pier N1 and on the northern part of the Main Span was completed in April 1994. The information obtained during this phase provided a general idea of the fundamental modes of vibration of the bridge. The work during the second phase, conducted in June 1994, concentrated on refining the mode shapes of the Main Span, on determining in which modes pier S1 had a significant participation, and on determining the fundamental modes of vibration of the South Approach structure between piers S2 and S5.

UBC's eight-channel accelerometer vibration measurement equipment and EDI's testing hardware and data analysis software were used to collect and analyze the ambient vibration data from more than 120 selected locations on the bridge and its foundations. Details of the AVS are described in Felber and Ventura [1]. The first nine experimentally determined natural frequencies and associated mode shapes of the Main Span are shown in Fig. 3. Plan views and elevation views of the inferred mode shapes are shown in the figure. The lowest frequencies are very close (0.46 Hz and 0.50 Hz) and the corresponding mode shapes are mainly a transverse mode and a longitudinal mode, respectively. All the modes determined experimentally include significant components in the vertical, transverse and longitudinal directions of the bridge. As a consequence, the calibration of the computer model of the bridge could be accomplished only through a three-dimensional dynamic analysis.

| Mode No. | Frequency (Hz) Exp. | Frequency (Hz) Anal. |
|---|---|---|
| 1 | 0.46 | 0.461 |
| 2 | 0.50 | 0.464 |
| 3 | 0.68 | 0.670 |
| 4 | 0.84 | 0.795 |
| 5 | 0.87 | 1.089 |
| 6 | 1.07 | 1.129 |
| 7 | 1.08 | 1.073 |
| 8 | 1.18 | 1.197 |
| 9 | 1.37 | 1.229 |

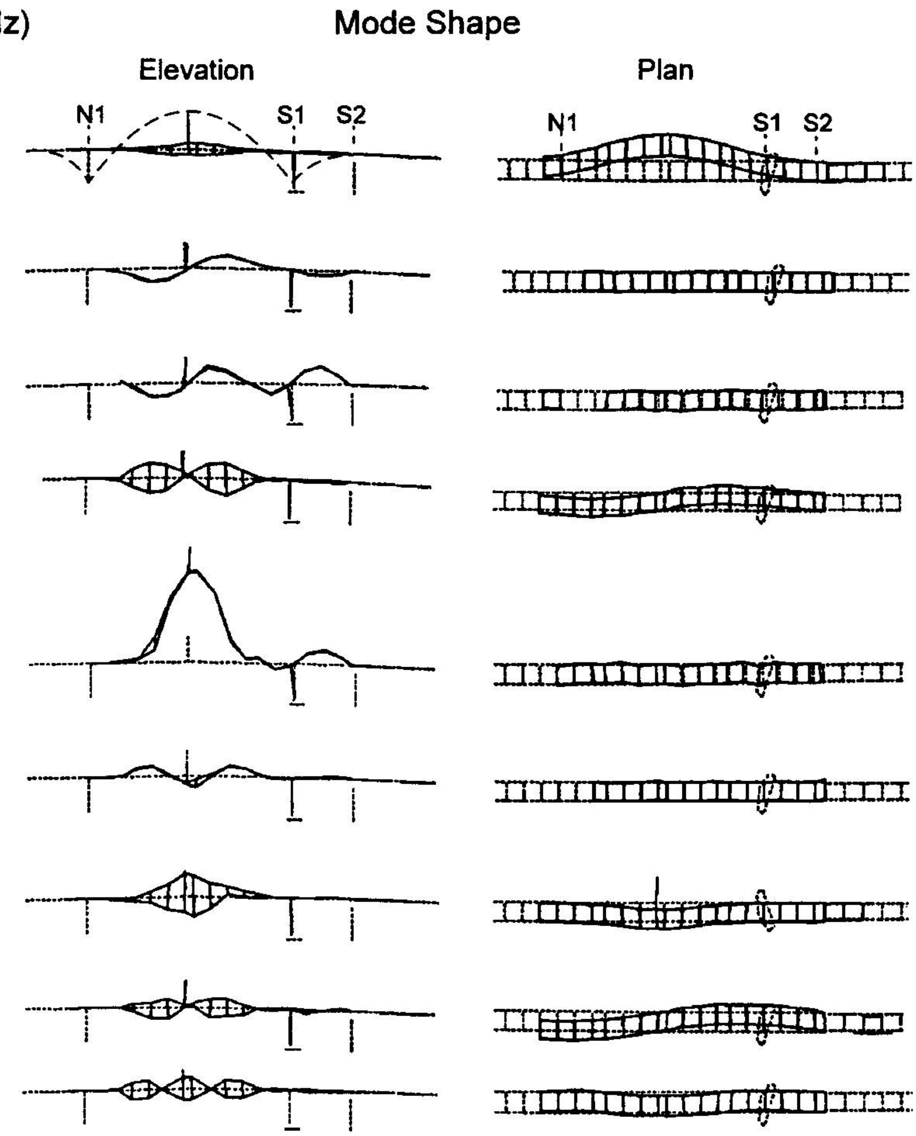


**Fig. 3 First Nine Natural Modes of the Main Span of Port Mann Bridge**

## 4. ANALYTICAL MODEL

Although the bridge might seem to be a relatively simple structure to model, critical assumptions regarding fixities and boundary conditions had to be made. A very important part of the modelling process was to establish realistic and accurate foundation stiffness parameters. Since the mass of the piers of the Main Span was far in excess of the structure itself, it was expected that modelling of the foundations would be a crucial part of the analysis. All the members of the Main Span were modelled as linear beam elements with the moments of inertia, torsional constants and masses derived from construction drawings. A spine member along the centre of the bridge was introduced to model the orthotropic deck.

For the approach spans, the concrete deck was modelled as equivalent cross braces while all the other members, including the reinforced concrete bents were represented as linear beam elements. Based on the AVS results, the interface (or bearings) between the superstructure and the piers were modelled as pins on pier N1 and S1, and as rollers permitting longitudinal translation for piers N2, S2. Bearings at S1 were designed as rollers, but appeared to be jammed according to the AVS results. For the approach spans, all the bearings were attached to the support bents and were allowed to move longitudinally, but were restrained to move in the transverse direction. The bridge foundations were modelled as linear springs with six components (three axial and three rotational). The spring stiffnesses were derived from soil data provided by the geotechnical consultant.

A layout of the bridge model and a closer view of the Main Span are shown in Fig. 4. The finite element linear elastic dynamic analysis was conducted first using B&T's finite element program CAMIL in order to calibrate the model and subsequent seismic assessment studies. CAMIL's calibrated model was subsequently analyzed with the commercially available program SAP90 [6] on a 486-PC computer. Details of the computer modelling and results are given by Ventura et al, [5].

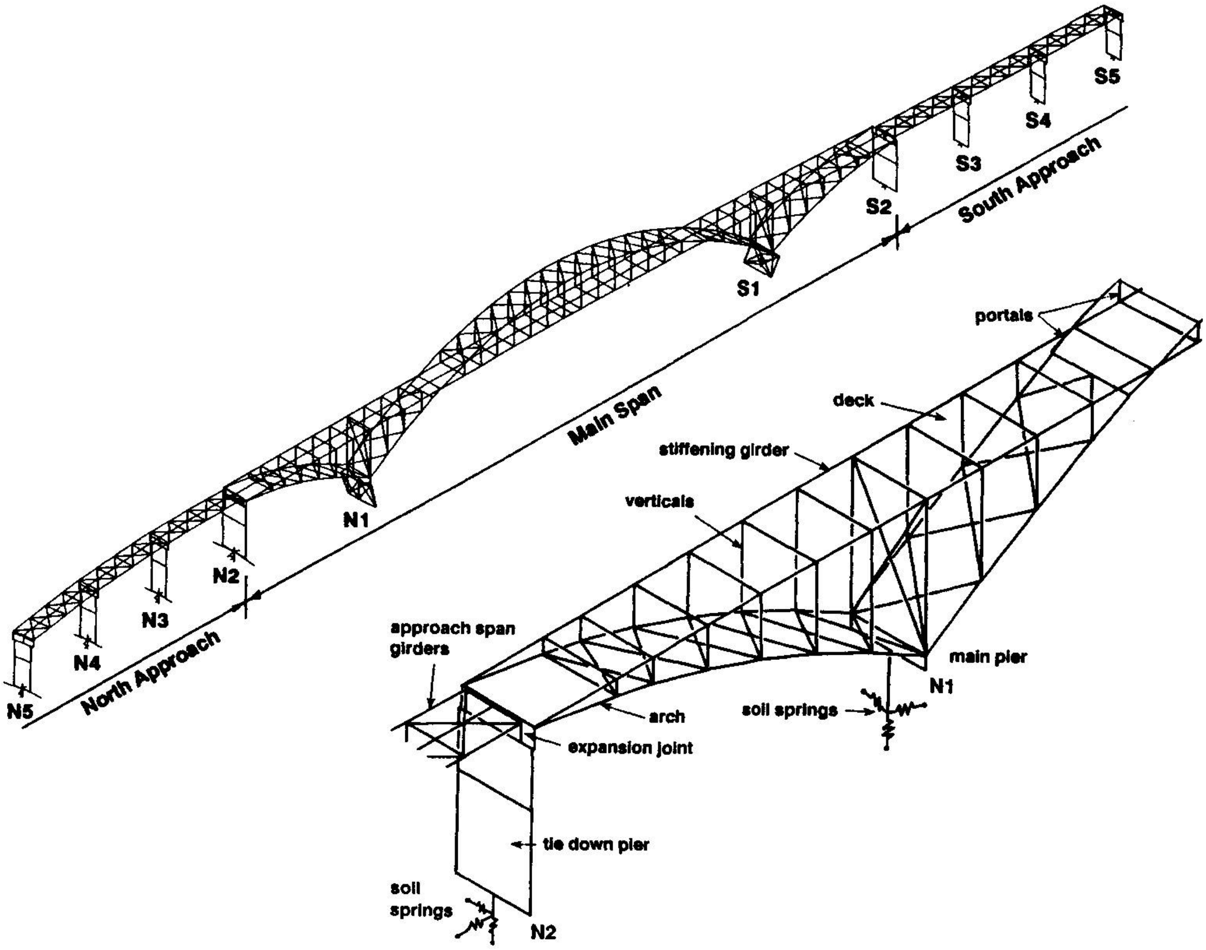


**Fig. 4 Finite Element Model of Port Mann Bridge**

The fundamental frequencies of the calibrated model correlated well with the experimental frequencies and are shown in Fig. 3. The associated mode shapes matched very well the experimental modes, but are not shown here due to space limitations.

The sensitivity of the model dynamic properties to the selection of the equivalent foundation springs was investigated by increasing and decreasing the spring constants determined by the geotechnical consultant. It was found that more than a tenfold variation of the spring constants would be needed to induce significant changes on the computed mode shapes and frequencies. It was concluded, therefore, that a very detailed refinement of the estimated spring constants was not warranted for the model calibration.

Additional studies included determination of the equivalent spring constants using the results from the AVS. The simple model shown in Fig. 5 was used to determine the values of the translational, $K_t$, and rotational, $K_r$, stiffnesses as a function of the measured motions along the height of the pier and at the foundation level. Using the recorded data, the relative values of the bending, $d_b$, rotational, $d_r$, and translational, $d_t$, components of the pier motion at its lowest natural frequency were determined. These values were used to compute the spring constants in terms of the flexural stiffness of the pier. The resulting spring constants were $K_t$=4.2x10$^5$ kN/m and $K_r$= 3.9x10$^8$ kN·m/rad. Considering the simplicity of this approach, these values compare reasonably well with those provided by the geotechnical consultant for low strain levels of the soil, $K_t$=10x10$^5$ kN/m and $K_r$= 1.6x10$^8$ kN·m/rad. No further refinements were attempted to improve this correlation.

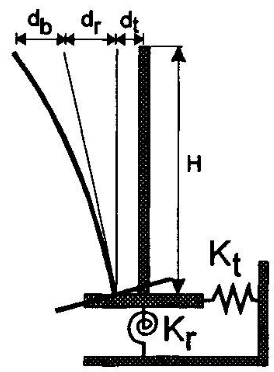


**Fig. 5 Pier-Foundation Model**

Because the experimental work was limited to measuring vibrations of the Main Span and part of the South Approach, not all the modes of vibration of the complete bridge could be properly identified and correlated with the finite element model. The correlation study presented here was limited to the first nine measured modes of the Main Span, which did not necessarily correspond to the first nine modes of the complete bridge model. Nevertheless, because of the large number of secondary modes, the correlation between the experimental and analytical study proved to be a crucial step in gaining insight and confidence about the dynamic characteristics of the bridge.

## 5. CONCLUSIONS

Correlation between the analysis and the model was not achieved initially because the boundary conditions indicated on the drawings did not agree with the actual behaviour of some bearings (S1). Also, some structural members of the bridge were found to be different from what was indicated on the drawings. Once these differences were accounted for, good agreement between measured modes and the computer model could be achieved. The information obtained from the ambient vibration testing helped the consulting engineers increase their confidence on the computer bridge model and significantly reduced the uncertainties on the analyses that came after, including the assessment of the soil-structure interaction effects for different levels of ground shaking.

## ACKNOWLEDGEMENTS

The support and cooperation of the Ministry of Transportation and Highways of British Columbia for this project is gratefully acknowledged.

## REFERENCES

1. FELBER, A.J. and VENTURA, C.E., Port Mann - Modal Testing and Model Correlation; Part I: Experimental Testing and Modal Analysis. Procs. of the 13th Int. Modal Analysis Conf., Nashville, Tennessee, February, 1995.
2. GOLDER, H.Q. and WILLEUMIER, G.C., Design of the Main Foundations of the Port Mann Bridge. The Engineering Journal, The Journal of the Engineering Institute of Canada, August, 1964.
3. HARDENBERG, G., Design of the Superstructure of the Port Mann Bridge. The Engineering Journal, The Journal of the Engineering Institute of Canada, July 1961.
4. LAKE, G.W.C., The Port Mann Bridge. Engineering Institute of Canada Annual Meeting Paper, 1964.
5. VENTURA, C.E., FELBER A.J. PRION, H.G.L., TAYLOR, P.R., and VAN SELST, A., Port Mann - Modal Testing and Model Correlation; Part II: Dynamic Modelling and Correlation. Procs. of the 13th Int. Modal Analysis Conf., Nashville, Tennessee, February 1995.
6. WILSON, E.L. and HABIBULLAH, A., SAP90 Structural Analysis Manual. Computer and Structures, Inc., Berkeley, California, 1992.

# Maintenance Inspection and Monitoring of Segmental Bridges

## Contrôle de la maintenance et surveillance des ponts à voussoirs préfabriqués

## Wartungs-Inspektion und Überwachung von Segmentbrücken

**Randall W. POSTON**
Vice President
KCI Technologies, Inc.
Manassas,VA, USA

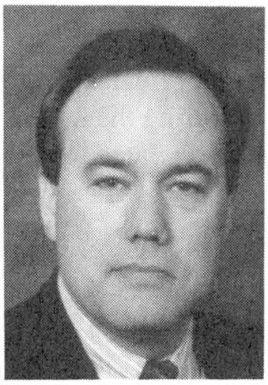

Randall W. Poston received his Ph.D. in structural engineering from the University of Texas at Austin in 1984. He is a past recipient of the ASCE T.Y. Lin Award and the Collingwood Prize. Dr. Poston serves as Chairman of ACI Committee 224 - Cracking.

**Keith KESNER**
Project Engineer
KCI Technologies, Inc.
Manassas,VA, USA

Keith Kesner received his B.S. in civil engineering from the University of Connecticut in 1992. He has three years' experience in evaluation and repair of concrete structures. He specialises in non-destructive testing of concrete structures.

**SUMMARY**

Dynamic load-testing of three retrofitted externally post-tensioned segmental bridges in the Washington Metropolitan Area Transit Authority heavy-rail system was conducted as part of a continuing integrity monitoring program. Results from dynamic testing are compared with benchmark values from previous testing. The development of a maintenance inspection manual for the structures is summarised.

**RÉSUMÉ**

Les essais de charge dynamique de trois ponts à voussoirs préfabriqués, renforcés par précontrainte extérieure appartenant au Réseau de transport public de la région de Washington, furent menés conformément au programme de surveillance continue des ouvrages concernés. Les résultats des essais dynamiques sont comparés aux valeurs-repères obtenues lors des essais précédents. L'élaboration d'un manuel d'inspection et de maintenance des structures y est aussi abordée.

**ZUSAMMENFASSUNG**

Dynamische Tragfähigkeitsproben von drei neu verstärkten äusserlich vorgespannten Segmentbrücken im Washington Areal Bahnsystem wurden durchgeführt als Teil eines kontinuierlichen Einheits-Überwachungsprogramms. Resultate von den dynamischen Proben wurden verglichen mit Massstabswerten von vorhergehenden Proben. Die Entwicklung eines Wartungsinspektionshandbuch für diese Brücken wird hier zusammengefasst.

## 1. HISTORY OF STRUCTURES

In the process of expanding Metrorail services further into Fairfax County, Virginia (USA), the Washington Metropolitan Area Transit Authority (WMATA) approved a value engineering change proposal in June, 1986, to substitute simply supported, single cell, external tendon, segmental box girders for three (3) continuous, twin cell, cast-in-place box girders. The substitute structures, collectively referred to as the J-2e bridge structures, include the Cameron Run Bridge (three spans of 33.5m, 39.6m, and 33.5m), Eisenhower Bridge (two spans each 33.5m), and the Van Dorn Street Bridge (two spans, each 30.5m).

Erection of the three bridge structures began during October , 1987. By February, 1988, significant cracking was observed in the diaphragm of all pier segments. In addition, three tendon deviator saddles of the Cameron Run Bridge were damaged during the longitudinal post-tensioning. Web concrete on the exterior of the Van Dorn Street structure was later reported to have delaminated at a pier segment.

Due to the observed distress in the J-2e bridge structures, an independent consultant evaluated the distress in the J-2e bridge structures and reviewed the proposed methods for repairing the structures. The consultant's report [1] identified and addressed four primary concerns related to the bridges, which reflected the concerns of WMATA at that time:

1) Cracking of pier-segment diaphragms and their strength
2) Cracking in tendon deviations and evaluation of retrofit measures
3) Delamination of web concrete in pier segments
4) Long-term behavior of bridge structures.

During the Spring and Summer of 1989, redesign of the damaged and undamaged tendon deviators were performed and a retrofit scheme for the pier segment diaphragms in two of the three bridges was designed. The pier-segment retrofit was initiated early in the Summer of 1989. In late 1989, based upon the recommendations of the independent consultant, additional modifications and additions to the retrofit of the pier segments was installed.

Based upon the performance history of the J-2e structures, the independent consultant recommended [1] that a series of static and dynamic load tests be performed on the structures. It was recommended that both a short- and long-term testing program be initiated to monitor the integrity of the J-2e structures.

As an outgrowth of those recommendations, a comprehensive static load test program and a follow-up dynamic load test were conducted the Fall of 1990 and Summer of 1991, respectively [2]. Based upon the favorable finding from the comprehensive short-term test program on the repaired structures, the WMATA Blueline which contains the J-2e structures opened for revenue operation on June 15, 1991.

Based upon favorable results from the short-term testing program, the original recommendation was relaxed from the prescribed annual inspection and second and fifth year comprehensive static load testing, to a program of annual inspection and less extensive testing during the second and fifth year of service for the purpose of monitoring the integrity of the retrofitted J-2e aerial structures.

Consistent with the previous recommendations, WMATA selected KCI Technologies, Inc. to conduct the second year revenue operation monitoring and inspection of the J-2e structures in 1993. The second year inspection and testing program examined the structural integrity of the aerial structures through a program of real-time dynamic testing consistent with the previous recommendations.

As a parallel task to conducting the second year testing and inspection program, a maintenance inspection manual was developed by KCI Technologies, Inc. for the J-2e structures. The development of this maintenance inspection manual was needed because of the uniqueness of the externally post-tensioned segmental construction of the J-2e structures in the WMATA bridge inventory, the unusual cracking experienced by the structures and the retrofit procedure implemented. The maintenance inspection manual was developed to provide guidelines and procedures for WMATA personnel to follow during their routine inspection of the J-2e structures.

## 2. SECOND YEAR DYNAMIC LOAD TEST PROGRAM

In the static load testing conducted in Fall 1990 [2], the J-2e structures were subjected to full design service loads including the effects of centrifugal forces, rolling forces and dynamic impact. This testing simulated the rare event of two fully loaded inbound and outbound trains passing over the same span simultaneously. The information taken during the initial static load testing serves as a benchmark for revenue operation monitoring of the J-2e structures at future points in its service life.

Analysis of the static load tests clearly indicated that the structures were behaving as linear-elastic, uncracked concrete structures. Thus, the basic premise by which the structures were evaluated for the second year testing program was that the behavior should be linearly proportional to the behavior observed during the static load test program and nearly identical to that measured during the first month of revenue operation since the trains generally had very light passenger loads, and generally only one train was crossing the bridge at any given time. The basic proportion of expected load during the second year monitoring was approximately 30% of that measured during the program of static load testing.

### 2.1 Instrumentation and Testing

Real-time measurements of the aerial structures as revenue trains passed over the span required the use of a high-speed field data acquisition system. A sampling rate of 100Hz was used in the testing since preliminary dynamic analysis revealed the predominant structural modes were well below 50Hz [3].

Real-time measurements were conducted for each bridge span independently. Field testing provided real-time strain readings at the bottom of the top flange and the top of the bottom flange. Accelerations were monitored at the longitudinal and transverse centerline of the midspan box segments.

During the testing program, elevation and tilt meter readings were taken on all spans. Elevation readings were used to determine the midspan camber of the bridge spans. Any significant decrease in camber from previously recorded benchmark values would signal a loss of effective prestressing, and thus a decrease in structural integrity.

2.2 Analysis Models

Based on the results from the static load test program, it was reasonable to assume that the measured structural behavior during the dynamic testing would also be linear-elastic and proportional. Accordingly, any significant loss of structural integrity would be signaled by a deviation from this premise.

It was anticipated that the principal structural response of a simply supported span subjected to a moving point axle load was from the fundamental mode of vibration [3]. Accordingly, a single-degree-of-freedom (SDOF) dynamic analysis model was used for general comparison purposes. An in-house computer program that calculates the response of a structural system using a frequency domain analysis was used to perform the analysis. The field monitoring during dynamic testing provided real-time strain readings at the bottom of the top flange and the top of the bottom flange. For evaluation purposes, an expression was derived for computing the strain versus time from the SDOF dynamic analysis. For the assumed shape function of

$$\phi\,(x) = \sin\frac{\pi x}{L},$$

the theoretical strain, $\epsilon$, in the concrete box section at midspan as a function of time can be shown to be as follows:

$$\epsilon\,(x = L/2,\, t) = \frac{\pi^2 y}{L^2}\,Y(t)$$

where

y = distance from the neutral axis

L = span length

and Y(t) = displacement with time computed from the SDOF dynamic analysis.

2.3 Comparison of Test Results with Analyses

A comparison of longitudinal strain histories measured in the 1993 test program to the upper and lower bound strains measured during the short-term load testing program conducted in Fall 1991 is shown in Figure 1. The measured strain in the second year testing program is slightly greater (~ $3\mu\epsilon$) than the upper bound measured during the earlier benchmark test program. In all probability, this is probably due to the increased passenger load on the trains compared to the virtually zero passenger load when the Blueline extension opened in 1991.

Figure 1 also shows the percentage (30%) of the strain measured in the static load test program in Fall 1990 with full design live loads. The measured strains are slightly higher than the 30% value which is based upon no passenger load. From a review of Figure 1 and examination of other data collected during the 1993 testing program [3], it is clearly evident that the response after two years of service is virtually identical to values established during the benchmark load testing program. This indicates that there has been no measurable loss of prestressing, which translates into no loss of structural integrity. Comparison of measured acceleration records also shows very close correlation to calculated values [3].

Midspan camber measurements for all three bridges have increased slightly with time ($\approx$ 2.5mm to 5 mm). This slight increase in the J-2e structures is due to long-term creep effects and is normal. These measurements provide additional data that indicate that there has been no measurable loss of prestressing.

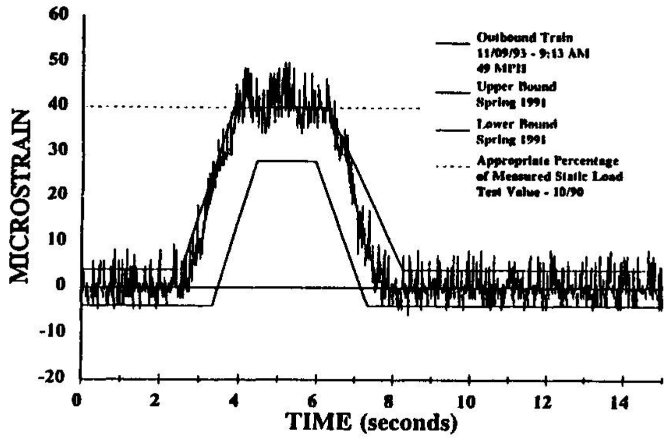


Fig. 1 Comparison of longitudinal strains measured on bottom of 39.6m Cameron Run span

## 3. MAINTENANCE INSPECTION MANUAL

### 3.1 Development of Manual

To insure long-term serviceability, durability and integrity, it is recognized that the J-2e structures would require a program of on-going maintenance and inspection. To the extent that KCI could determine, there are no known standards for inspection of existing post-tensioned concrete segmental bridges. Accordingly, the maintenance inspection manual was developed to provide WMATA inspection forces with appropriate guidance to insure the continued safety, long-term serviceability and durability of the J-2e structures [4].

### 3.2 Elements Addressed

The J-2e structures are currently one of only a few post-tensioned, segmental structures in the WMATA inventory. This, coupled with the unique nature of distress exhibited by various structural components and the attendant retrofit procedures implemented, necessitated a detailed structural element inventory be included in the maintenance inspection manual.

The maintenance inspection manual provides WMATA personnel with detailed description of the elements and their function in the structure. Element descriptions are backed up by photographs and drawings that identify the individual components to the inspectors. Also included in the manual are appendices which indicate the location of all existing cracks in the structures and the location of previously repaired items. These appendices serve as a condition benchmark for the structures. Guidelines are included in the manual that provide acceptable levels of variation from benchmark values for measured quantities such as midspan chamber.

3.3 Review Checklist/Element Rating

The procedure for inspection of the J-2e structures is laid out in a flow chart, as seen in Figure 2 [4], which identifies the items to be inspected at each structural element. Any observed defects are recorded on checklist sheets. Individual checklist sheets are used for condition assessments of existing repairs and for camber determination and bearing pad movement.

All elements assessed by the inspection team are assigned a numerical rating (0-5 scale, with 5 indicating good condition) to assess their condition. Upon completion of the inspection all items rated 3 or below must be reviewed by a WMATA Engineer. Additionally, the entire inspection package, including all checklists, must be reviewed by the Engineer to complete the inspection of the J-2e structures. This system will allow the inspection to be conducted by WMATA field personnel with a built in review by a WMATA Engineer.

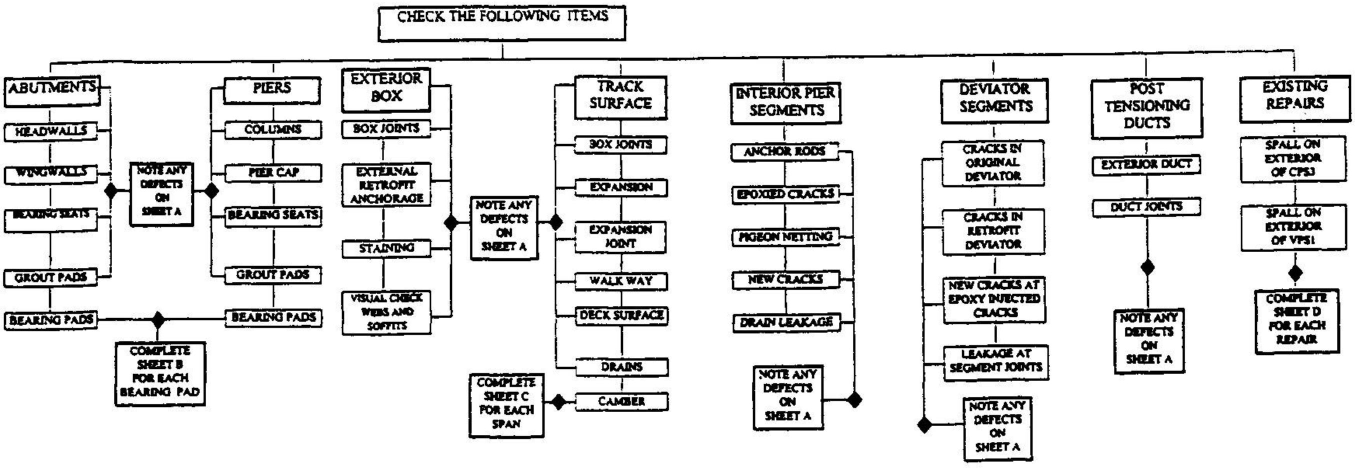


Fig. 2 Flowchart used for inspection of J-2e Aerial Structures

REFERENCES

1. KREGER, M.E., "Evaluation of Distress in J-2e Bridge Structures", Report to DeLeuw, Cather & Company and Washington Metropolitan Area Transit Authority, November, 1989.

2. POSTON, R. W. and IRSHAD, M., "Load Test Evaluation of Externally Post-Tensioned Segmental Box-Girder Aerial Structures", ACI Third International Concrete Bridge Symposium, March, 1992.

3. "Report on Second Year Inspection and Revenue Operation Monitoring of the J-2e Aerial Structures", Report submitted by KCI Technologies, Inc. to Washington Metropolitan Area Transit Authority, 600 Fifth Avenue, NW, Washington, D.C. 20001, December, 1993.

4. "J-2e Aerial Structures Maintenance Inspection Manual", Manual submitted by KCI Technologies, Inc. to Washington Metropolitan Area Transit Authority, 600 Fifth Avenue, NW, Washington, D.C., 20001, December, 1993.